Multilayering and Loss of Apical Polarity in MDCK Cells Transformed with Viral K-*ras*

Cora-Ann Schoenenberger, Anna Zuk, Donna Kendall, and Karl S. Matlin

Department of Anatomy and Cellular Biology, Harvard Medical School, Boston, Massachusetts 02115

Abstract. The effects of viral Kirsten *ras* oncogene expression on the polarized phenotype of MDCK cells were investigated. Stable transformed MDCK cell lines expressing the v-K-*ras* oncogene were generated via infection with a helper-independent retroviral vector construct. When grown on plastic substrata, transformed cells formed continuous monolayers with epithelial-like morphology. However, on permeable filter supports where normal cells form highly polarized monolayers, transformed MDCK cells detached from the substratum and developed multilayers. Morphological analysis of the multilayers revealed that oncogene expression perturbed the polarized organization of MDCK cells such that the transformed cells lacked an apical–basal axis around which the cytoplasm is normally organized. Evidence for selective disruption of apical membrane polarity was provided by immunolocalization of membrane proteins; a normally apical 114-kD protein was randomly distributed on the cell surface in the transformed cell line, whereas normally basolateral proteins remained exclusively localized to areas of cell contact and did not appear on the free cell surface. The discrete distribution of the tight junction–associated ZO-1 protein as well as transepithelial resistance and flux measurements suggested that tight junctions were also assembled.

These findings indicate that v-K-*ras* transformation alters cell-substratum and cell-cell interactions in MDCK cells. Furthermore, v-K-*ras* expression perturbs apical polarization but does not interfere with the development of a basolateral domain, suggesting that apical and basolateral polarity in epithelial cells may be regulated independently.

EPITHELIAL cells are organized into sheets of contiguous cells that line free surfaces of organisms, forming boundaries between external and internal compartments (Berridge and Oschman, 1972). Epithelia both protect the organism and regulate the environment of the compartments they separate (for reviews, see Simons and Fuller, 1985; Rodriguez-Boulan and Nelson, 1989).

In simple epithelia, each cell displays a distinct polarized organization which determines the overall morphology of the monolayer. The apical plasma membrane of epithelial cells is typically organized into microvilli (Simons and Fuller, 1985; Rodriguez-Boulan and Nelson, 1989). The closely apposed lateral membranes of adjacent cells engage in cell-cell interactions which maintain the continuity of the monolayer. In particular, they form intercellular junctions that are arranged in a specific sequence (Farquhar and Palade, 1963). The tight junction, or zonula occludens, is located at the apex of lateral membranes between neighboring cells and thus marks the transition from apical to basolateral membrane (for reviews, see Gumbiner, 1987; Madara and Hecht, 1989). By limiting the flow of solute through the paracellular pathway, tight junctions contribute substantially to the epithelial permeability barrier (for review, see Powell, 1981). They may also play a role in the establishment and maintenance of the polarized phenotype (van Meer and Simons, 1986; Gumbiner, 1987). Below the tight junction is the zonula adherens, followed by desmosomes and gap junctions. The basal surface of polarized cells abuts a basement membrane and interacts with components of the extracellular matrix. The structural polarization of the cell surface domains extends to the spatial organization of the cytoplasm. The centrosome and Golgi complex, for example, tend to be found in a supranuclear position in the apical part of the cell, whereas the nucleus resides more basally (Fawcett, 1986). Other cytoplasmic organelles and the cytoplasmic and cortical cytoskeletons are also spatially organized with respect to the apical–basal axis (Fawcett, 1986; Wilson, 1987).

The diverse vectorial functions of epithelia in solute and protein transport require the organization into cohesive monolayers as well as in the polarized distribution of proteins and lipids between the apical and basolateral domains (Simons and Fuller, 1985; Rodriguez-Boulan and Nelson, 1989). Depending on the cell type, specific proteins are localized to only one domain of the plasma membrane. In most epithelial cells, the Na^+,K^+-ATPase, for example, is located in the basolateral domain (Louvard, 1980), whereas other proteins, such as the amiloride sensitive Na^+ channel, are predominantly expressed on the apical surface (Simons and

1. *Abbreviation used in this paper*: IM, inulin.

Fuller, 1985; Rodriguez-Boulan and Nelson, 1989). In addition, the restriction of several plasma membrane antigens of unknown function to specific domains has been demonstrated using mAbs (Balcarova-Ständer et al., 1984; Hertzlinger and Ojakian, 1984). The unique protein and lipid composition is generated by sorting membrane components along specialized transport pathways to their respective domains and preventing the components of the distinct domains from becoming intermixed (Caplan and Matlin, 1989).

The mechanisms involved in the development and maintenance of epithelial cell surface polarity are not well understood. The establishment of polarity has been studied during mouse embryogenesis; there, nonpolarized blastomeres of the preimplantation embryo acquire cell surface polarity in response to increased cell–cell contacts (Flemming and Johnson, 1988). Similarly, the conversion of embryonic kidney mesenchyme to epithelial cells is triggered by cell adhesion proteins such as laminin and uvomorulin (Ekblom, 1989). These studies suggest that cell-substratum and cell-cell interactions are important inducers of polarization (Rodriguez-Boulan and Nelson, 1989).

Further insight into the mechanisms of polarization in vitro has been gained from studies using the MDCK epithelial cell line. Recent results indicate that cell–cell and cell–substratum contact have distinct roles in the morphogenesis of polarized epithelia (Wang et al., 1990). For instance, the generation of an apical pole seems to be initiated by an asymmetric external signal. Upon attachment of MDCK cells to a substratum in the absence of cell-cell contacts, apical proteins are present on the free cell surface only, whilst the distribution of basolateral markers remains unpolarized (Vega-Salas et al., 1987*a*,*b*; Ojakian and Schwimmer, 1988). For the induction of basolateral polarity, however, cell–cell contacts are required (Nelson and Veshnock, 1986, 1987*a*,*b*; Vega-Salas et al., 1987*a*). It is likely, thus, that independent mechanisms may be involved in the establishment of basolateral and apical domains.

Despite the importance of cell polarity to every epithelial function, it has not been the focus of any study on epithelial transformation in vitro. Introduction of oncogenes into a variety of epithelial cell lines repeatedly changes their phenotype and growth properties, and renders them tumorigenic in nude mice (Darfler et al., 1986; Rijsewijk et al., 1987; Warren and Nelson, 1987; Ball et al., 1988; Redmond et al., 1988). However, the effects on apical–basolateral organization are not considered. It is conceivable that the breakdown of polarity may be a critical step in carcinogenesis in vivo, since cell–cell and cell–substratum contacts, determinants of polarity in normal epithelia, need to be disrupted for tumor progression to ensue (Behrens et al., 1989; for review, see Nicolson, 1989).

In this study, we examine the effects of oncogenic transformation on the organization and polarity of MDCK cells. We find that when grown on permeable substrata, MDCK cells expressing the v-K-*ras* gene display perturbed cell adhesion properties resulting in the formation of multilayers. The abrogation of the monolayer is accompanied by the loss of the apical-basal axis and the breakdown of structural polarity in multilayered cells. Oncogenic *ras* expression disrupts apical polarity only; an apical membrane protein is randomly distributed over the entire cell surface in transformed MDCK cells, whereas basolateral proteins remain exclusively localized to areas of cell contact. These findings suggest that basolateral and apical polarity may be regulated independently.

Materials and Methods

Cells

To limit cell heterogeneity of the parental cell line, MDCK cells were cloned by limiting dilution from an MDCK stain II stock (low transmonolayer resistance; Matlin and Simons, 1983) before infection. After three rounds of cloning, a subclone was chosen on the basis of its cuboidal morphology, its growth rate, its ability to form domes, and its transepithelial resistance. Passage 6 of this subclone was used for infection experiments. To minimize effects related to clonal variation, experiments using infected cells were performed at passages <15.

MDCK cells and transformed cell lines were grown in MEM supplemented with Earle's salts, 5% FBS, 10 mM Hepes, pH 7.3 (complete medium), at 37°C in 95% air/5% CO_2 (Matlin and Simons, 1983). Cells were harvested by trypsin-EDTA (Gibco Laboratories, Grand Island, NY) treatment for 30 min at 37°C, and subcultured at appropriate dilutions. Medium components were purchased from Gibco Laboratories and Sigma Chemical Co. (St. Louis, MO) and sterile plasticware was from Falcon Labware (Oxnard, CA). For studies of cells on permeable supports, cells were plated at 6×10^4 cm^{-2} on Millicell HA filters (0.45 μm pore size; Millipore Corp., Bedford, MA), Millicell PCF filters (0.4 μm pore size; Millipore Corp.) or Transwells (0.4 μm pore size; Costar Corp., Cambridge, MA). Filter-grown cells were cultured for the time indicated with daily medium changes.

The pA317 packaging cell line (American Type Culture Collection, Rockville, MD; No. CRL 9078; Miller and Buttimore, 1986) was grown in DME with high glucose (4.5 g/liter) supplemented with 10% FBS.

Vector Construction

The pMV-7 retroviral vector has been described elsewhere (Kirschmeier et al., 1988). Plasmid constructions and DNA manipulations were performed according to standard protocols (Maniatis et al., 1982). Eco RI linkers were added to a Hinc II–Stu I fragment encoding the v-K-*ras* oncogene (Ellis et al., 1981), which was then inserted into the unique Eco RI site of the pMV-7 vector. In this construct, designated pMV-7K*ras* (Fig. 1), the transition start codon of the oncogene was located ~550 bp downstream from the transcription start site in the viral 5′-long terminal repeat. Restriction enzymes, T4 DNA ligase, and DNA linkers were purchased from Boehringer-Mannheim Biochemicals (Indianapolis, IN), Pharmacia Fine Chemicals (Piscataway, NJ) or New England Biolabs (Boston, MA).

Retroviral Infection of MDCK Cells

The pA317 packaging cell line was used to produce helper-free replication defective retroviruses (Miller and Buttimore, 1985). 60-mm cultures dishes of 50–80% confluent pA317 cells (seeded 12 h earlier) were transiently transfected with 10 μg pMV-7 or pMV-7K*ras* recombinant plasmid DNA via the calcium-phosphate precipitation technique (Graham and van der Eb, 1973; Wigler et al., 1979). Culture supernatants containing recombinant virus were collected 36–48 h after transfection and filtered through 0.45-μm Millex-HA filters (Millipore Corp.).

MDCK cells (5×10^5) were plated in 60-mm dishes 12 h before infection. To infect, the medium was removed and 1 ml of filtered pA317 virus supernatant was added in the presence of 8 μg/ml polybrene (Aldrich Chemical Co., Milwaukee, WI) and incubated for 24 h at 37°C. Then 2 ml complete medium with 8 μg/ml polybrene was added. After 24 h, cultures were split into selective medium containing 0.6 mg/ml G418 (Gibco Laboratories). Selection medium was replaced every 4 d. After 10 d of selection, single colonies were isolated with cloning rings and subcloned twice by limiting dilution.

Influenza Virus Infection

Control and transformed MDCK cell lines grown on Millicell-HA or Transwell filters were infected with influenza virus strain A/PR/8/34 (H1 subtype; PR8) as described (Matlin and Simons, 1984). Filters were processed for frozen sectioning (see below) 6 h after infection, and for ultrastructural analysis (see below) 10 h after infection.

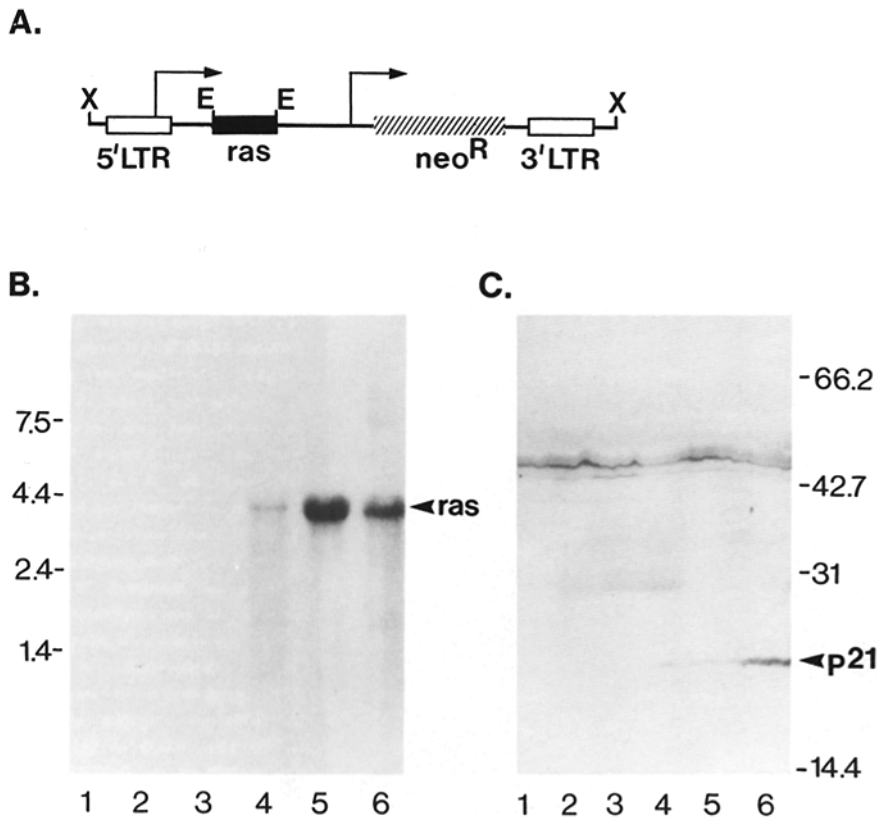

Figure 1. Oncogene expression in v-K-*ras*-transformed MDCK cells. (*A*) Schematic representation of the v-K-*ras*-containing pMV-7 retroviral vector. To insert the oncogene into pMV-7, Eco RI linkers were ligated to a Hinc II–Stu I fragment encoding the v-K-*ras* gene (*ras*) and then cloned into the Eco RI (*E*) restriction site of pMV-7. The resulting pMV-7K*ras* construct is flanked by the long terminal repeats (*LTR*) of the Moloney murine sarcoma virus and contains the drug resistance gene neo^R under the regulation of the herpes simplex thymidine kinase promoter. The start of the 5'LTR promoted oncogene transcript and the tk-neo^R transcript are indicated by arrows. The predicted length of a 5'LTR controlled oncogenic transcript is ~3.9 kb. MDCK cells were infected with the pMV-7 retroviral vector alone, lacking the *ras* gene (control) or the oncogenic pMV-7K*ras* retroviral construct. *E*, Eco RI; *X*, Xho I. (*B*) Expression of pMV-7K*ras* mRNA in transformed MDCK cells lines. Northern blot analysis was performed on 10 μg of total RNA isolated from parental (lane *1*), pMV-7 control (lanes *2* and *3*), and pMV-7K*ras*-transformed (lanes *4–6*) MDCK cell lines. Blots were probed with v-K-*ras* sequences. A predominant oncogenic transcript of ~3.9 kb was detected in MDCK cells transformed with pMV-7K*ras*. The locations of RNA size markers (in kilobases) are shown on the left. Lane *1*, parental MDCK; lane *2*, pMV-7 control cell line C2; lane *3*, pMV-7 control cell line C6; lane *4*, pMV-7K*ras* transformed MDCK cell line R2; lane *5*, pMV-7K*ras*-transformed MDCK cell line R3; lane *6*, pMV-7K*ras*-transformed cell line R5. (*C*) Immunoblot analysis of protein from untransformed and transformed MDCK cell lines with mAbs recognizing *ras* protein. Protein was extracted from cells grown on plastic substrata and 150 μg were separated in each lane on a 10% SDS gel, and transferred to Immobilon. Proteins were analyzed by reacting the blot with mAb Y13-259, followed by secondary goat anti-rat IgG antibodies conjugated to alkaline phosphatase. p21-*ras* protein encoded by the pMV-7K*ras* construct was detected in the transformed MDCK cell lines. Lane *1*, parental MDCK; lane *2*, pMV-7 control cell line C2; lane *3*; pMV-7 control cell line C6; lane *4*, pMV-7K*ras*-transformed MDCK cell line R2; lane *5*, pMV-7K*ras* transformed MDCK cell line R3; lane *6*, pMV-7K*ras*-transformed cell line R5. Molecular mass standards (in kilodaltons) are indicated on the right.

RNA Analysis

Total RNA from cells grown on plastic dishes was extracted by the guanidine isothiocyanate method (Chirgwin et al., 1979). Single-stranded DNA probes were radiolabeled with ^{32}P by random primed labeling (Boehringer-Mannheim Biochemicals). For Northern blotting, equivalent amounts of RNA were denatured at 65°C for 5 min with formaldehyde and formamide, electrophoresed on 1% agarose gels containing 2.1% formaldehyde, transferred to nylon membranes (HyBond-N; Amersham International, Arlington Heights, IL), and UV cross-linked to the membrane (Davis et al., 1986). Blots were hybridized overnight at 65°C with a radiolabeled *ras* or actin probe in 0.75 M Na_2HPO_4, pH 7.2, containing 5% SDS, then washed at 65°C in 0.3 M Na_2HPO_4, pH 7.2, containing 1% SDS, and exposed at −70°C to Kodak XAR-5 film with intensifying screens. Signal intensities were quantified by densitometry using an Ultro Scan XL-enhanced laser densitometer (Pharmacia LKB Biotechnology Inc., Gaithersburg, MD). Multiple exposures were taken of each blot to allow for linearity in the x-ray film response.

Antibodies

Rat mAb R40.76 against ZO-1, a peripheral membrane protein specific for tight junctions (Anderson et al., 1988) was obtained from D. A. Goodenough (Harvard Medical School, Boston); the mouse anti-uvomorulin mAb (rr1; Gumbiner and Simons, 1986) was provided by B. Gumbiner (University of California, San Francisco); the rat anti-*ras* mAb (Y13-259; Furth et al., 1982) was obtained from J. B. Gibbs (Merck, Sharp, & Dohme Research Laboratories, West Point, PA); the mouse monoclonal antibodies recognizing the 114-kD apical protein and the 58-kD basolateral protein were a gift from K. Simons (European Molecular Biology Laboratory, Heidelberg) and have been described previously (Balcarova-Ständer et al., 1984); the mouse mAb H28-E23 against hemagglutinin was obtained from W. Gerhart and J. Yewdell (Wistar Institute, Philadelphia). Affinity-purified secondary antibodies were purchased from Tago Inc. (Burlingame, CA; FITC-conjugated goat anti-rat IgG, FITC- or rhodamine-conjugated goat anti-mouse IgG + IgM) and from Amersham International (Texas Red-linked sheep anti-mouse Ig).

Protein Extraction and Immunoblotting

Membrane fractions were prepared from monolayers of untransformed and transformed MDCK cells at 4°C in the presence of protease inhibitors (10 μg/ml aprotinin; 1 mM PMSF, 17 μg/ml benzamidine, 1 μg/ml pepstatin, 1 μg/ml antipain, and 1 mM iodoacetamide). The cells were rinsed twice with ice-cold homogenization buffer (250 mM sucrose in 10 mM Tris, pH 7.4), scraped from the Petri dish in the same buffer (1 ml/10-cm plate), and homogenized with a ball bearing homogenizer (clearance 4 μm). Cell breakage was confirmed under the microscope. After adjusting the sucrose concentration to 1.4 M with 2.3 M sucrose in 10 mM Tris, pH 7.4, homogenates (10 ml/tube) were overlaid with homogenization buffer and centrifuged at 4°C in an SW 40.1 rotor (Beckman Instruments, Inc., Fullerton, CA) for 1 h at 83,000 *g* (25,600 rpm). Membrane-enriched interfaces were removed, washed in homogenization buffer, and centrifuged at 4°C in a 50 Ti rotor (Beckman Instruments) for 30 min at 95,500 *g* (32,500 rpm). Pellets were suspended in 2% SDS, 5 mM EDTA, pH 8.0, 200 mM Tris,

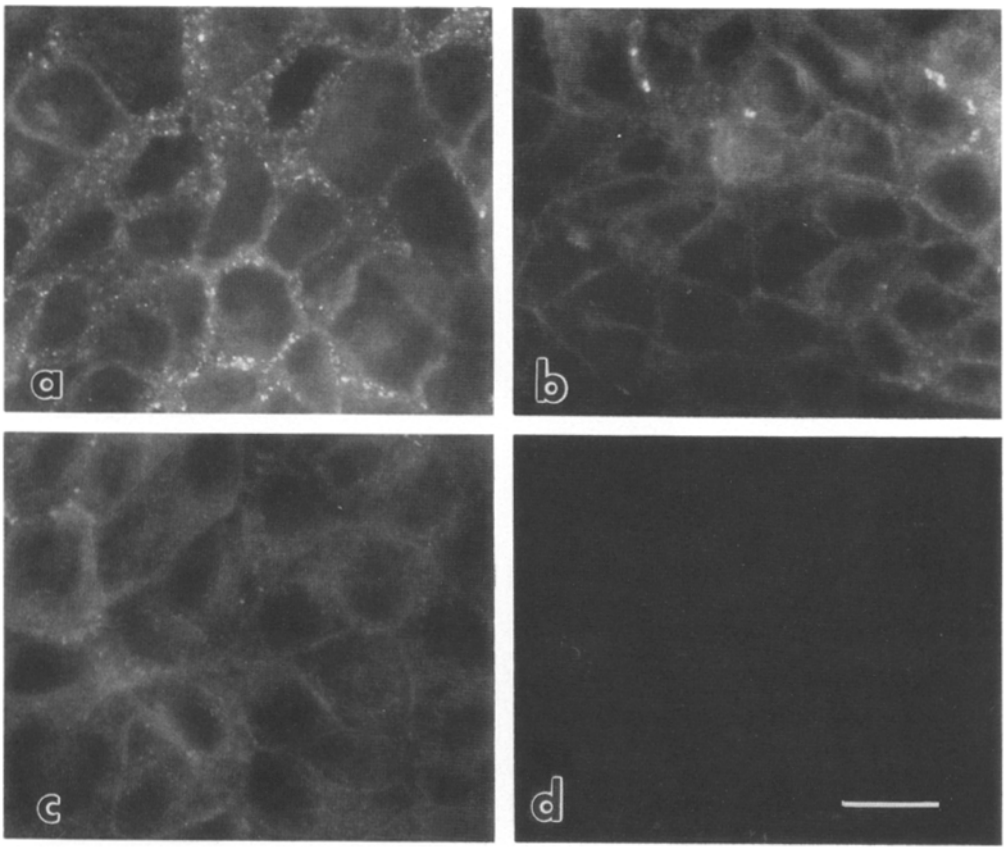

Figure 2. Immunolocalization of pMV-7Kras protein in transformed MDCK cell lines. Cells on glass coverslips were grown to confluency, fixed in PLP, permeabilized and incubated with anti-*ras* mAbs (Y13-259) followed by FITC-coupled anti-rat secondary antibodies. All cell lines were stained in parallel and photographic processing was identical. Staining is punctate and predominantly localized to the cell periphery in all transformed cell lines. The signal was most intense in R5 cells (*a*), slightly reduced in R3 (*b*), weak in R2 cells (*c*). Little or no staining was detected in C6 control cells (*d*). Bar, 20 μm.

pH 8.8, and frozen in liquid nitrogen. Protein samples were stored at −80°C.

Electrophoresis of proteins on 10% SDS polyacrylamide gels was performed according to the method of Laemmli (1970). The amount of protein in each sample was determined by a sensitive Coomassie blue dye binding assay (Bramhall et al., 1969). Equal amounts of protein were separated in each lane. Proteins were electrophoresed from SDS polyacrylamide gels to Immobilon membranes (Millipore Corp.) in transfer buffer (25 mM Tris, 200 mM glycine, 20% methanol, 0.1% SDS) for 2 h at 12 V with the Genie apparatus (Idea Scientific, Corvallis, OR). Blots were processed as described by Burke et al. (1982) using 1:450 diluted anti-*ras* Y13-259 antibody as primary and 1:1000 diluted goat anti-rat IgG conjugated to alkaline phosphatase (Pierce Chemical Co., Rockford, IL) as secondary antibody. The enzymatic activity was revealed by color development in 100 mM Tris, pH 9.5, 100 mM NaCl, 5 mM $MgCl_2$ containing nitroblue tetrazolium (3.3 mg/10 ml) and 5-bromo-4-chloro-3-indolyl phosphate (1.65 mg/10 ml).

Immunofluorescence

Indirect immunofluorescence was performed either on cells grown on coverslips or on cryosections of filter-grown cells.

Coverslips. Cells were grown to confluency on glass coverslips and rinsed with PBS, pH 7.4, containing 1 mM $CaCl_2$ and 0.5 mM $MgCl_2$ (PBS^+). For staining with Y13-259, cells were fixed for 20 min at room temperature with a freshly prepared solution of 2% paraformaldehyde, 75 mM L-lysine, and 10 mM $NaIO_4$, pH 7.2 (PLP fixative; McLean and Nakane, 1977), rinsed in PBS^+ and quenched with 50 mM NH_4Cl in PBS^+. After rinsing with PBS^+, cells were permeabilized with 0.1% Triton X-100 in PBS^+ for 4 min. Alternatively, coverslip cultures were fixed and permeabilized with methanol for 10 min at −20°C (for staining with rrl).

Nonspecific binding sites were blocked with 0.2% gelatin in PBS (blocking buffer) for 30–60 min. Coverslips were incubated successively with primary and corresponding secondary antibodies for 30–45 min with extensive washing in PBS and blocking buffer after each incubation. All incubations were performed in a humidified atmosphere at room temperature. Coverslips were mounted in PBS containing 0.1% *N,N,N',N'*-tetramethyl-p-phenylene diamine (to limit bleaching of the fluorochrome), 90% glycerol, and viewed with a Zeiss Axiophot Microscope equipped with epifluorescence illumination. All images were recorded with TMAX-400 film (Eastman Kodak Co., Rochester, NY).

Semi-thin Frozen Sections. To view antigen distribution along the apical-basolateral axis, immunofluorescence was performed on cryosections of cells cultured in either Millicell PCF or Transwell filter chambers. Cultures were rinsed with PBS^+ and fixed with PLP for 1 h at 4°C. After washing with PBS, filters were excised from the plastic holders and cut into small segments of ~1 mm^2. For embedding, segments were incubated for 10 min at 37°C in 10% bovine skin gelatin in PBS and transferred to 4°C to solidify the gelatin. Gelatin-embedded filter segments were postfixed for 30 min at 4°C with PLP and rinsed with PBS. They were then infiltrated with 2.1 M sucrose for 2 h at room temperature, mounted on specimen holders, and rapidly frozen by immersion in freon precooled with liquid nitrogen, followed by immersion in liquid nitrogen. Semi-thin frozen sections (~0.5 μm) were cut on an Ultracut FC4D microtome (Reichert-Jung, Vienna, Austria) at −80°C. Sections were collected in 2.3 M sucrose and transferred to coverslips previously coated with 0.05% chromium potassium sulfate in 0.5% bovine skin gelatin. Sections were stored at −20°C for up to 1 wk before use. Staining of sections on coverslips was as described for cells on coverslips. In addition, nuclei were counterstained with 0.5 μg/ml Hoechst no. 33258 (Sigma Chemical Co.) for 10 min at room temperature, followed by thorough washing in PBS.

Electron Microscopy

For ultrastructural analysis, cells were grown in Millicell HA filters for eight days, rinsed with PBS^+ and fixed for 1 h at room temperature in 2.5% glutaraldehyde, 2% paraformaldehyde in 0.1 M cacodylate buffer, pH 7.4. Filters were excised from the plastic holders, cut into small pieces and osmicated (1% OsO_4 in 0.1 M cacodylate buffer) for 60 min at 4°C. Filter segments were then stained en bloc with 1% uranyl acetate for 1 h at room temperature. Specimens were dehydrated in ethanol and propylene oxide and embedded in Epon-Araldite. Sections were cut on an Ultracut FC4D microtome (Reichert-Jung) or a Sorvall MT2-B ultramicrotome (DuPont Instruments, Wilmington, DE). Semi-thin plastic sections (0.5–1 μm) were stained with 0.25% toluidine blue in 0.5% sodium borate and viewed with

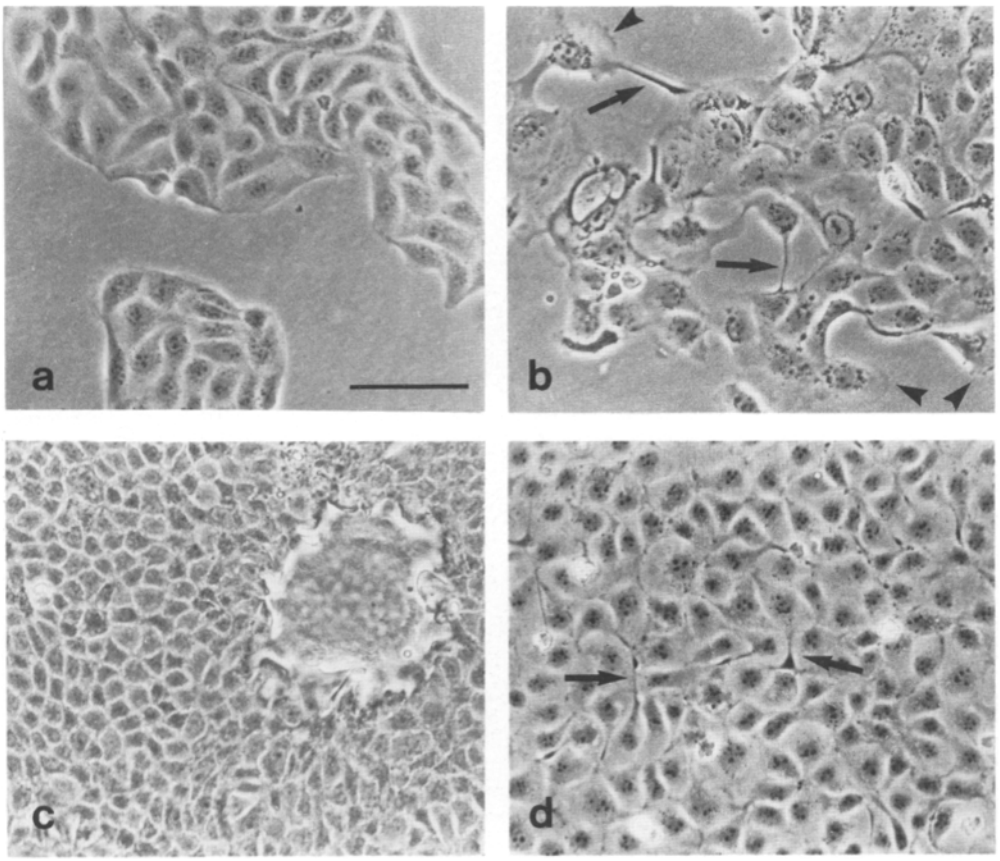

Figure 3. Phase morphology of R5 transformed and C6 control MDCK cell lines on plastic substratum. Cells were subcultured on plastic petri dishes and photographed at subconfluent (*a* and *b*) and saturation density (*c* and *d*) with phase-contrast optics. (*a*) At subconfluency, the C6 control cell line forms islands with smooth borders. (*b*) In subconfluent R5 cultures, transformed cells display processes (*arrows*) and membrane ruffling (*arrowheads*). (*c*) C6 at saturation density; monolayer with cobblestone appearance and characteristic dome formation. (*d*) R5 at saturation density; continuous monolayer. Note that compared with the untransformed control cells the saturation density of R5 is clearly reduced and domes do not occur. Cell shape is reminiscent of the normal epithelial phenotype, but cells appear to extend processes (*arrows*) over neighboring cells. Bar, 100 μm.

a Zeiss Axiophot. Thin sections were stained with 0.2% lead citrate and observed on a JEOL 100CX electron microscope.

Transepithelial Electrical Resistance and Flux Measurements

The functional integrity of tight junctions was assayed by (*a*) measuring the resistance of cells grown on Millicell HA tissue culture inserts to the transepithelial passage of current (Cereijido et al., 1981; Madara and Dharmsathaphorn, 1985; Madara and Hecht, 1989), and (*b*) measuring the rate of transfer of ^{14}C-inulin from the apical to basolateral compartment of the Millicell HA chamber (Madara and Dharmsathaphorn, 1985; Madara and Hecht, 1989).

Resistance measurements were performed with the Millicell Electrical Resistance System (Millipore Corp.) according to the manufacturer's specifications. Transepithelial electrical resistances were calculated after subtracting the background contributed by a blank filter.

To assess inulin leak across 8 d filter cultures, Millicell HA inserts in 24-well tissue culture plates were rinsed twice with serum-free medium, followed by serum-free medium containing 0.5 mM inulin (IM; Sigma Chemical Co.) and incubated for 10 min with matching IM fluid levels (315 μl apical and 625 μl basolateral). All solutions were prewarmed at 37°C, and incubations were at 37°C in a 5% CO_2–95% air atmosphere with gentle agitation. After 10 min, the apical solution was replaced with inulin-medium containing 0.2 μCi ^{14}C-inulin/ml (New England Nuclear, Boston, MA). Cultures were returned to the incubator for 45 min, then 300 μl aliquots were collected periodically from the basolateral compartment and rapidly replaced with prewarmed IM. Aliquots were counted in a liquid scintillation counter (Beckman Instruments).

Results

Establishment of v-K-ras Transformed MDCK Cell Lines

To establish MDCK transformants, the viral Kirsten *ras* oncogene was stably introduced into an early passage of an MDCK II subclone by retroviral infection. The transducing retroviral construct used to generate helper-free virus is shown in Fig. 1 *A*. The v-K-*ras* oncogene was cloned into the unique Eco RI site of the pVM-7 retroviral vector (Kirschmeier et al., 1988). In this construct, transcription of the oncogene is controlled by the 5′ long terminal repeat of the Moloney murine sarcoma virus. In addition, pMV-7 contains the selectable drug resistance gene *neo* under the regulation of the internal herpes simplex virus thymidine kinase promoter. Replication-defective virions used to infect MDCK cells were produced by the packaging cell line pA317 (Miller and Buttimore, 1986; see Materials and Methods). Control cell lines were generated by introducing the pMV-7 vector without the *ras* oncogene insert into MDCK cells. MDCK cells with proviral insertions were selected in G418-containing medium. A number of neo^R colonies were isolated and subcloned by limiting dilution. The insertion of a single copy of the proviral genome of the expected structure was demonstrated by restriction digestion (data not shown). Three transformants, designated R2, R3, and R5, which represent independent proviral integration events, were chosen for further characterization. Three independent control cell lines were established in parallel. They were indistinguishable with respect to morphology and growth characteristics, and the C6 line was used as representative control in most instances.

The expression of the v-K-*ras* oncogene in MDCK transformants was analyzed at the RNA and protein level. Northern blotting of RNA extracted from transformants and con-

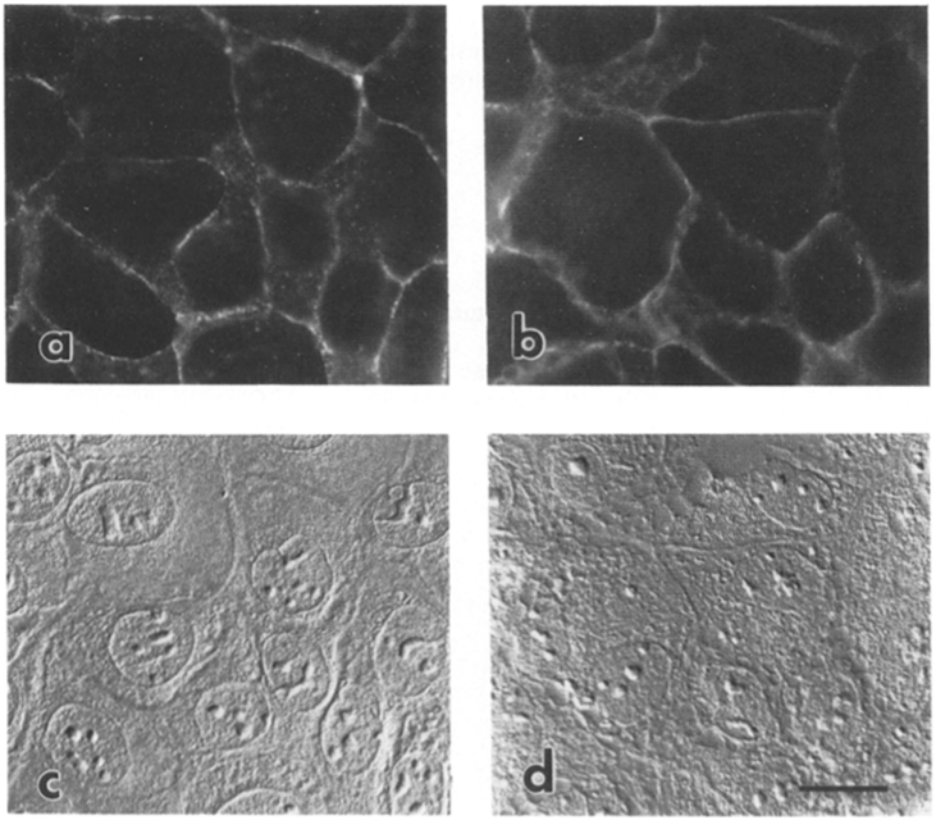

Figure 4. Immunolocalization of uvomorulin in monolayers of R5 transformants and control cells grown on coverslips. In *a* and *b*, methanol-fixed monolayers were incubated with a mouse mAb specific for uvomorulin (*rrl*) followed by Texas Red–tagged sheep anti–mouse Ig (1:30 dilution). Representative fields of cells were photographed. The same fields viewed under Nomarski optics are shown in *c* and *d*, respectively. Uvomorulin staining is localized predominantly to the contact zone between adjacent cells. (*a* and *c*) C6 control cell line; (*b* and *d*) R5-transformed cell line. Bar, 15 μm.

trol cell (C2 and C6) lines is shown in Fig. 1 *B*. The predicted size of a full-length transcript of the pVM-7K*ras* construct is ~3.9 kb. The probe used to analyze oncogene expression in MDCK transformants hybridized primarily to v-K-*ras* sequences; hybridization to the endogenous canine c-*ras* was not detectable under the experimental conditions shown in Fig. 1 *B*. To compare the levels of pMV-7K*ras* transcripts expressed in different clones, equivalent amounts of RNA were electrophoresed in each lane. R2 expressed the lowest levels of *ras* RNA, whereas levels in R3 and R5 did not differ significantly. These observations were confirmed by densitometric analysis of autoradiographs in which ratios of *ras* to actin signal intensities of individual lanes were compared (data not shown).

The synthesis of the oncogene encoded p21-*ras* protein was demonstrated by Western blotting (Fig. 1 *C*) using the rat mAb Y13-259 (Furth et al., 1982). The epitope recognized by this antibody lies in a highly conserved region (Barbacid, 1987), suggesting that the absence of a p21 band in the parental MDCK cells and in control cell lines is due to low levels of endogenous *ras* protein rather than lack of antibody crossreactivity. Consequently, the reactive band represents p21-*ras* protein encoded by the retroviral construct. The three transformants R2, R3, and R5 showed differential p21 expression. The low level of pMV-7K*ras* transcripts present in R2 was reflected by the amount of protein. The oncogene product was most abundant in R5 and intermediate levels were found in R3.

To immunolocalize the pMV-7K*ras* protein in the transformants, the clones and a control cell line were grown to confluency on glass coverslips and *ras* protein was visualized by indirect immunofluorescence (Fig. 2). Staining of transformed MDCK cells with Y13-259 revealed that *ras* protein was predominantly localized to the cell periphery. This distribution is consistent with the association of p21-*ras* with the inner leaflet of the plasma membrane (Willingham et al., 1980). The four cell lines shown in Fig. 2 were stained in parallel and the photographic processing was identical, thus allowing direct comparison of staining patterns. R5 (Fig. 2 *a*) showed most intense fluorescence whereas staining was least pronounced in R2 cells (Fig. 2 *c*). No staining was observed in the control cell line C6 (Fig. 2 *d*). Thus, the immunofluorescence data substantiated the immunoblotting results (Fig. 1 *C*).

The transforming potential of the oncogene product was examined by injecting MDCK transformants and control cell lines into nude mice. All transformed MDCK cell lines induced tumor formation within two weeks after injection. The tumor tissues expressed high levels of pMV-7K*ras* RNA (data not shown). The control cell lines failed to induce tumors even after an observation period of three months (Stiles et al., 1976*a*,*b*).

In summary, introduction of a v-K-*ras* gene into MDCK cells via retroviral infection yielded a number of transformed MDCK cell lines, each expressing a characteristic level of pMV-7*ras* mRNA and protein, and each of which proved tumorigenic in nude mice.

Morphology and Growth Properties of MDCK Transformants on a Solid Substratum

The morphology of pMV-7K*ras* expressing MDCK cells grown on plastic petri dishes was examined by phase microscopy (Fig. 3). At subconfluency, colonies of control cells displayed smooth borders (Fig. 3 *a*). However, R5 cells at low density did not grow as discrete colonies (Fig. 3 *b*). Instead,

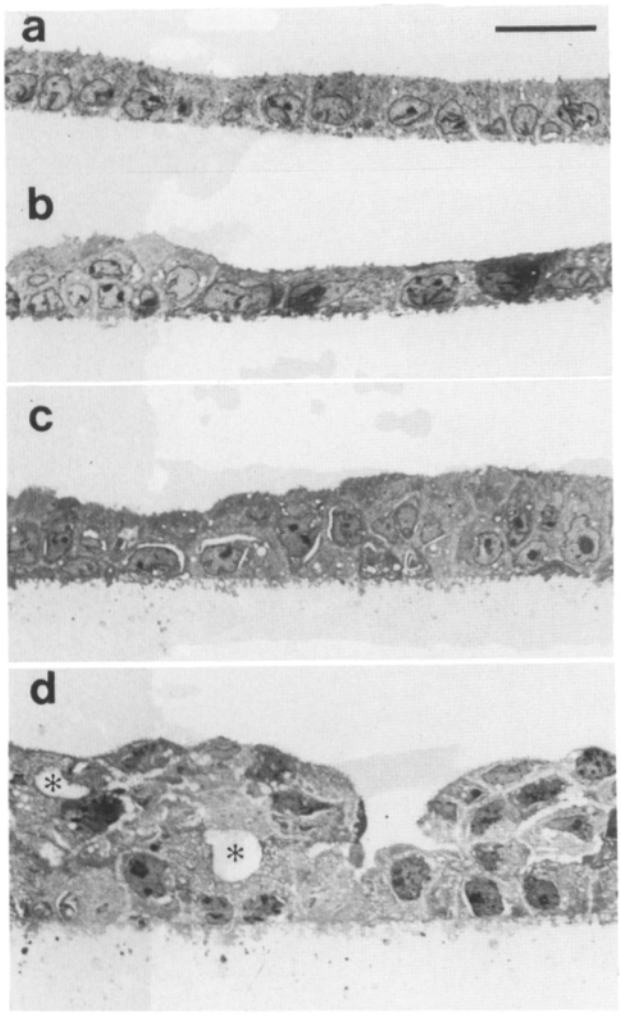

Figure 5. Transformed MDCK cells form multilayers on permeable supports. Control cells and transformed MDCK cell lines were plated at 1.7×10^5 cm^{-2} cells on Millicell HA filter chambers and cultured for 8 d. Micrographs of 1 μm plastic sections cut perpendicular to the filter are shown. (*a*) The control cell line C6 forms a regular monolayer of closely opposed cells. Blebbing into the filter at the basal surface is minimal. (*b*) R2 transformed cells cluster occasionally but the majority of the cells are organized into a polarized monolayer. (*c*) R3 transformants develop one to three layers of heteromorphic cells. (*d*) R5 cells form the most extensive multilayers with abundant blebbing of the cell surface contacting the filter. Lumena (*) were often seen within the multilayer. Bar, 20 μm.

in many cases they extended processes and showed extensive membrane ruffling, both indications of migratory activity (Abercrombie, 1980). When confluent, control cell lines displayed a cobblestone appearance typical of epithelial cells and formed domes (Fig. 3 *c*). These characteristics were indistinguishable from those of the parental MDCK clone. As shown in Fig. 3 *d*, transformation by v-K-*ras* did not entirely abrogate these normal properties; R5 cells retained the cuboidal shape to some extent and still formed continuous monolayers at high cell density. However, the processes observed in subconfluent R5 cultures were also evident in monolayers, where they appeared to extend over adjacent cells, and dome formation did not occur (Fig. 3 *d*). In addition, comparison of this cell line with the control cell line at saturation density (Fig. 3, *c* and *d*) suggested that R5 cells grew to a substantially lower cell density. This was confirmed by quantitative analysis of cell growth, which revealed a saturation density of $\sim 4 \times 10^5$ cm^{-2} for control cells, whereas R5 cells reached a saturation density of only 1×10^5 cm^{-2}. The growth properties of R2 and R3 transformants on plastic substrata were similar to each other, and more closely resembled those of the control cell line than did R5. While R2 cells occasionally formed domes as well as ridge-like structures at saturation density, only the latter were observed in R3 cultures.

Overall, these observations suggested that the growth characteristics of transformed MDCK cells on plastic substrata were altered by *ras* expression.

Uvomorulin Localizes to Regions of Cell–Cell Contacts in Transformed MDCK Cells

Establishment of the epithelial phenotype and the development of polarity are believed to depend on the expression of the cell adhesion molecule uvomorulin (Gumbiner et al., 1988; Ekblom, 1989; McNeill et al., 1990). In addition, absence of uvomorulin in transformed MDCK cells has been reported to be correlated with invasiveness (Behrens et al., 1989). Therefore, we investigated whether pMV-7K*ras* transformed MDCK cells express uvomorulin. Indirect immunofluorescence showed uvomorulin expression in C6 control cells and R5 transformants (Fig. 4, *a* and *b*). In both instances, the distribution of uvomorulin was similar; en face views showed staining mainly at the plasma membrane of cells that, by Nomarski interference contrast microscopy, appeared to be in contact (Fig. 4, *c* and *d*). Similar staining patterns were observed for R3 and R2 (data not shown).

MDCK Cell Transformants Detach from the Substratum and Form Multilayers when Cultured on Permeable Supports

It has been shown that culturing epithelial cells on permeable supports that permit separation of apical and basolateral compartments and expose the basolateral surface to the medium is conducive to the expression of a higher degree of differentiation than is growth on plastic (Valentich, 1982; Handler et al., 1984; Simons and Fuller, 1985; Fuller and Simons, 1986; Parry et al., 1987). The effect of such culture conditions on the epithelial organization of transformed MDCK cells was analyzed by culturing cells on Millicell HA filters. Fig. 5 shows vertical sections of transformed MDCK clones and C6 control cells. Control cells formed a homogeneous monolayer (Fig.5 *a*). R2 filter cultures (Fig. 5 *b*) grew predominantly as monolayers, but occasionally were disrupted by regions of cell clustering. Despite having growth properties on plastic similar to those of R2, R3 on permeable supports formed layers one to three cells thick, with cell morphology appearing more heterogeneous than in the R2 clone. Multilayering was most extensive in R5 transformants (Fig. 5 *d*). R5 cells, which showed reduced saturation density relative to control cells when grown on plastic, developed multilayers up to five layers thick after 8 d of culture on filters. Cell size and cell shape varied considerably and lumena were often seen within the multilayers. In addition, the three transformants exhibited more extensive blebbing into the filter on the basal surface of cells adjacent to the

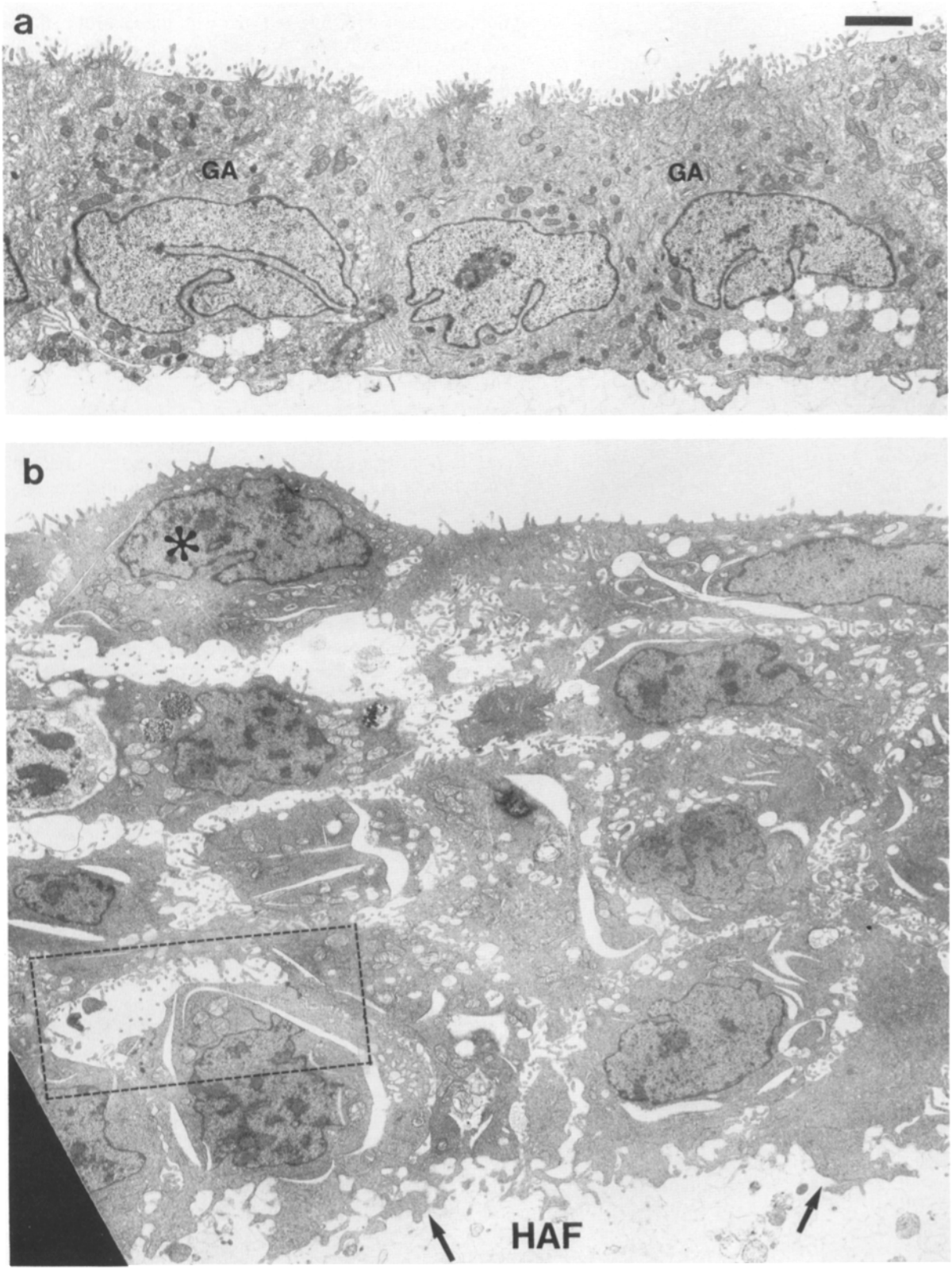

Figure 6. Electron micrographs of control monolayer and R5 multilayer. Ultrastructural analysis of control and R5 cells grown on Millicell HA filter chambers for 8 d showed that the distinct monolayer organization of normal MDCK is disrupted by transformation in R5 cells. (*a*) C6 control cells form a regular monolayer with cells structurally polarized along an apical–basal axis. Microvilli are abundant on the apical surface and the nuclei are located basally with the Golgi apparatus (*GA*) in a supranuclear position. Lateral membranes are closely apposed with junctional complexes between adjacent cells. (*b*) The apical–basal axis is not evident in multilayered R5 cells: microvilli on the free surface are reduced and nuclei are positioned randomly. Intercellular spaces are enlarged and spanned by prominent interdigitations. Note the extensive blebbing (*arrows*) of R5 cells into the Millicell HA filter (*HAF*). A higher magnification of the cell indicated by the asterisk and the boxed area are shown in Fig. 7, *a* and *b*, respectively. Bar, 2.5 μm.

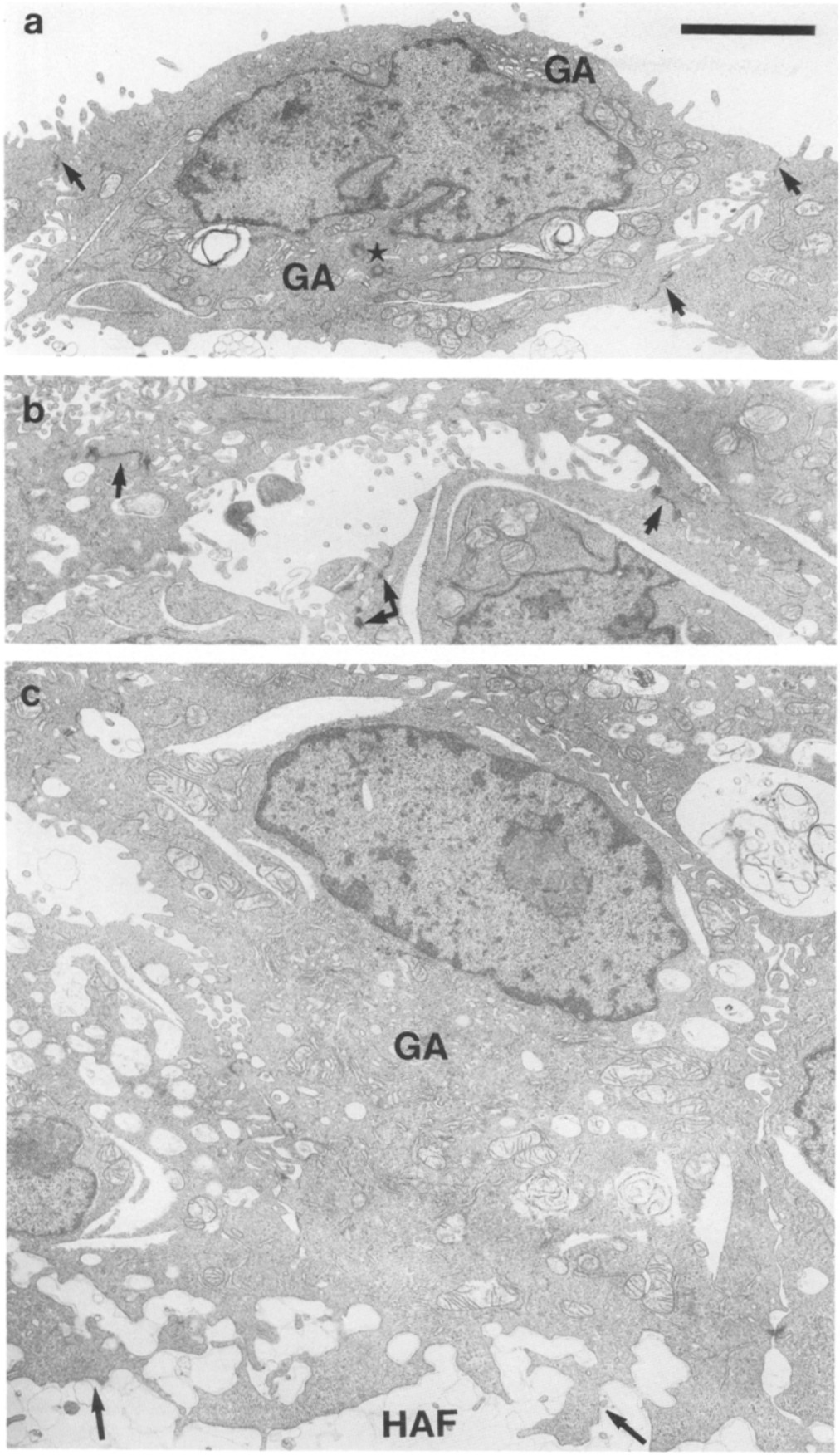

Figure 7. Structural polarity is absent in R5 cells. (*a*) Higher power electron micrograph of the cell in the uppermost layer shown in Fig. 6 *b*. The Golgi apparatus (*GA*) is located above and below the nucleus. The micrograph shows the centrosome in an atypical position beneath the nucleus (★). Microvilli on the free surface are sparse and cell processes resembling microvilli are apparent on the opposite cell surface. The junctional complexes between adjacent cells are indicated by arrows. (*b*) Electron dense structures (*arrows*) characteristic of junctional complexes are localized to boundaries of cells outlining the intercellular lumen boxed in Fig. 6 *b*. (*c*) Abundant Golgi stacks (*GA*) below the nucleus in a cell contacting the filter. In the top left corner a lumen and intercellular junctions are apparent. Arrows point to blebbing into the Millicell HA (*HAF*) filter. Bar, 2.5 μm.

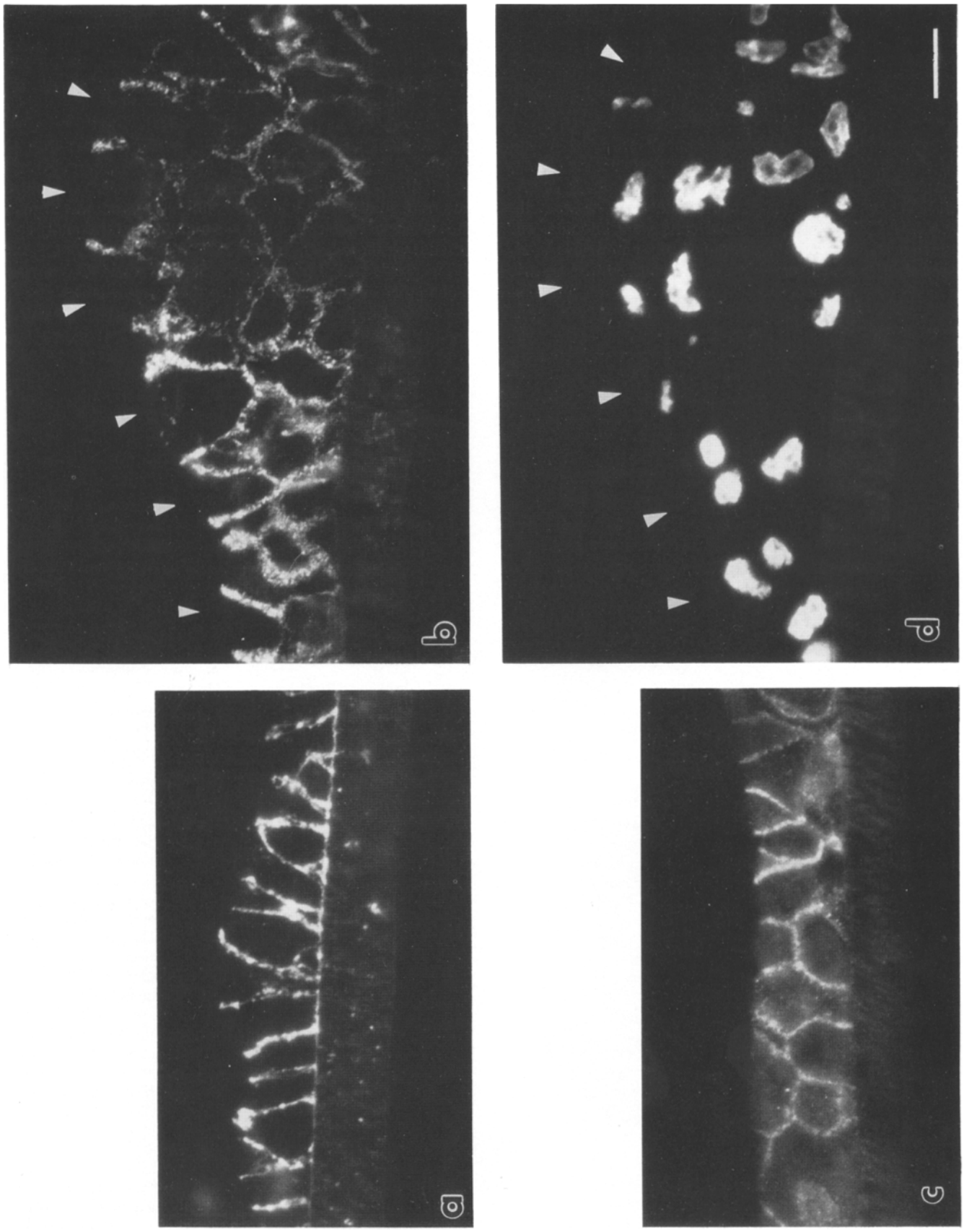
a
b
c
d

filter than control cells. As with multilayering, this was most evident with R5 cells.

The Apical–Basal Axis that Determines the Polarized Morphology of MDCK Cells Is Lost in Multilayered v-K-ras Transformants

When grown on permeable supports, normal MDCK cells display a highly polarized phenotype. Ultrastructural analyses revealed that the morphologic features of the C6 control cells (Fig. 6 *a*) were indistinguishable from those of the parental MDCK line. Individual cells were cuboidal and formed a regular monolayer with lateral membranes closely apposed. The apical surface was characterized by extensive microvilli. Tight junctions at the cell apex between neighboring cells demarcated the transition of apical to basolateral surface (Simons and Fuller, 1985; Fawcett, 1986). Additional components of the intercellular junctional complex were evident along lateral membranes of adjacent cells. The basal surface was attached to the filter and occasionally protruded into the underlying substratum. The asymmetry extended not only to specializations of the cell surface but also to the cytoplasm; nuclei tended to be located basally, whereas centrosomes and Golgi complexes resided supranuclear, towards the apical pole of the cell.

This structural polarization was clearly disrupted in the multilayered R5 cells (Fig. 6 *b*; Fig. 7). Although the top layer of cells facing the free surface still extended microvilli indicative of apical membranes, they were less abundant. In addition, membranes forming intercellular lumena within the multilayer also appeared to be organized into microvilli (Fig. 7 *b*). Cells within the multilayer also lacked a distinct apical pole and were surrounded by neighboring cells along their entire surface. The centrosome and Golgi complex had no definitive position relative to the nucleus and the substratum. For example, in the cell shown in Fig. 7 *a*, Golgi profiles were located apically and basally and also the centrosome was below the nucleus. Aberrant positioning of the Golgi complex was found even in cells that were attached to the filter, as shown by the extensive Golgi profiles located below the misplaced nucleus in Fig. 7 *c*. Spaces between R5 cells were prominent, suggesting that neighboring cells were not as closely apposed as in monolayers of control cell lines. However, the interdigitations spanning the intercellular spaces as well as the presence of distinct intercellular junctions provided evidence that cells in the multilayer were engaged in cell-cell contacts.

These morphological data indicate that pMV-7K*ras* expression resulted in the loss of the apical–basal axis around which polarized MDCK cells are organized. Unlike simple epithelia, filter-grown MDCK cell transformants do not stay attached to the substratum at their basal surface, but detach from the filter and form disorganized multilayers.

Transformation Disrupts Apical Polarity without Affecting the Distribution of Basolateral Markers

Our data showing that morphological aspects of polarization are disrupted by transformation were complemented by immunolocalization studies on the distribution of apical and basolateral surface markers. To view the localization of domain-specific proteins over the entire plasma membrane, semi-thin frozen sections (0.5–1 μm) were cut perpendicular to the filter and stained by indirect immunofluorescence. In addition, transverse sections of multilayers guaranteed that the surface of each cell within the multilayer was equally accessible to the reacting antibody.

The basolateral distribution of a 58-kD protein (Balcarova-Ständer et al., 1984) in filter-grown control cells is demonstrated in Fig. 8 *a*. Fluorescent staining was confined to areas of cell–cell and cell–substratum contacts and was absent from the apical surface. Similarly, the free cell surface in R5 multilayers was not labeled by the mAb against 58 kD (Fig. 8 *b*). Whether the staining within the multilayer represents basal localization of the 58-kD protein in the upper cell or aberrant localization of this protein in the contacting cell below cannot be discerned. However, the polarized distribution of the 58-kD protein in the top layer suggests that R5 cells retain a defined basolateral surface domain. A similar staining pattern was observed with mAbs to the Na^+,K^+-ATPase, which in untransformed MDCK cells is a marker for the basolateral membrane (data not shown; Louvard, 1980; Caplan et al., 1986). Furthermore, uvomorulin staining was also absent from the free cell surface and confined to regions of cell–cell contact (Fig. 8 *c*; Behrens et al., 1985; Gumbiner et al., 1988; Nelson et al., 1990; Wang et al., 1990).

To analyze the distribution of apical cell surface markers, cryosections of R5 multilayers were probed with an mAb recognizing a 114-kD apical protein (Balcarova-Ständer et al., 1984). As anticipated, this antibody stained the apical surface of control monolayers (Fig. 9 *a*). Little or no staining was detected along the basolateral membranes. In contrast, multilayered R5 cells were labeled by the anti-114-kD antibody along the entire cell surface (Fig. 9, *b* and *d*). The disruption of apical polarity was attenuated in R3 cells and the apical localization of the 114-kD protein was minimally affected in R2 cells (data not shown), suggesting that the disruption of apical polarity and the expression of pMV7K*ras* were related proportionally.

When polarized MDCK cells are infected with influenza virus, the viral spike glycoprotein hemagglutinin is segregated to the apical plasma membrane where virion assembly and budding take place (Rodriguez-Boulan and Sabatini, 1978). Thus, hemagglutinin and budding virions can be used as exogenous markers for the apical domain in normal cells. R5 cells infected with influenza virus revealed a randomized dis-

Figure 8. Distribution of basolateral membrane proteins in control and transformed MDCK cells. C6 and R5 cells grown for 8 d on Transwell filters were processed for indirect immunofluorescence as semi-thin (~0.5 μm) cryosections cut perpendicular to the substratum. Cryosections were stained with mAbs to a 58-kD protein specific for the basolateral membrane domain (*a* and *b*) or with monoclonal antibodies to the cell adhesion protein uvomorulin (*c*). *a* shows the basolateral localization of the 58-kD protein in C6 monolayers. In R5 multilayers (*b*) the 58-kD protein is also excluded from the free cell surface (outlined by *arrowheads*). The position of the nuclei in this section is revealed by the DNA-binding fluorochrome Hoechst 33258 (*d*). Uvomorulin staining (*c*) in R5 multilayers is also confined to areas of cell–cell contact. Bar, 10 μm.

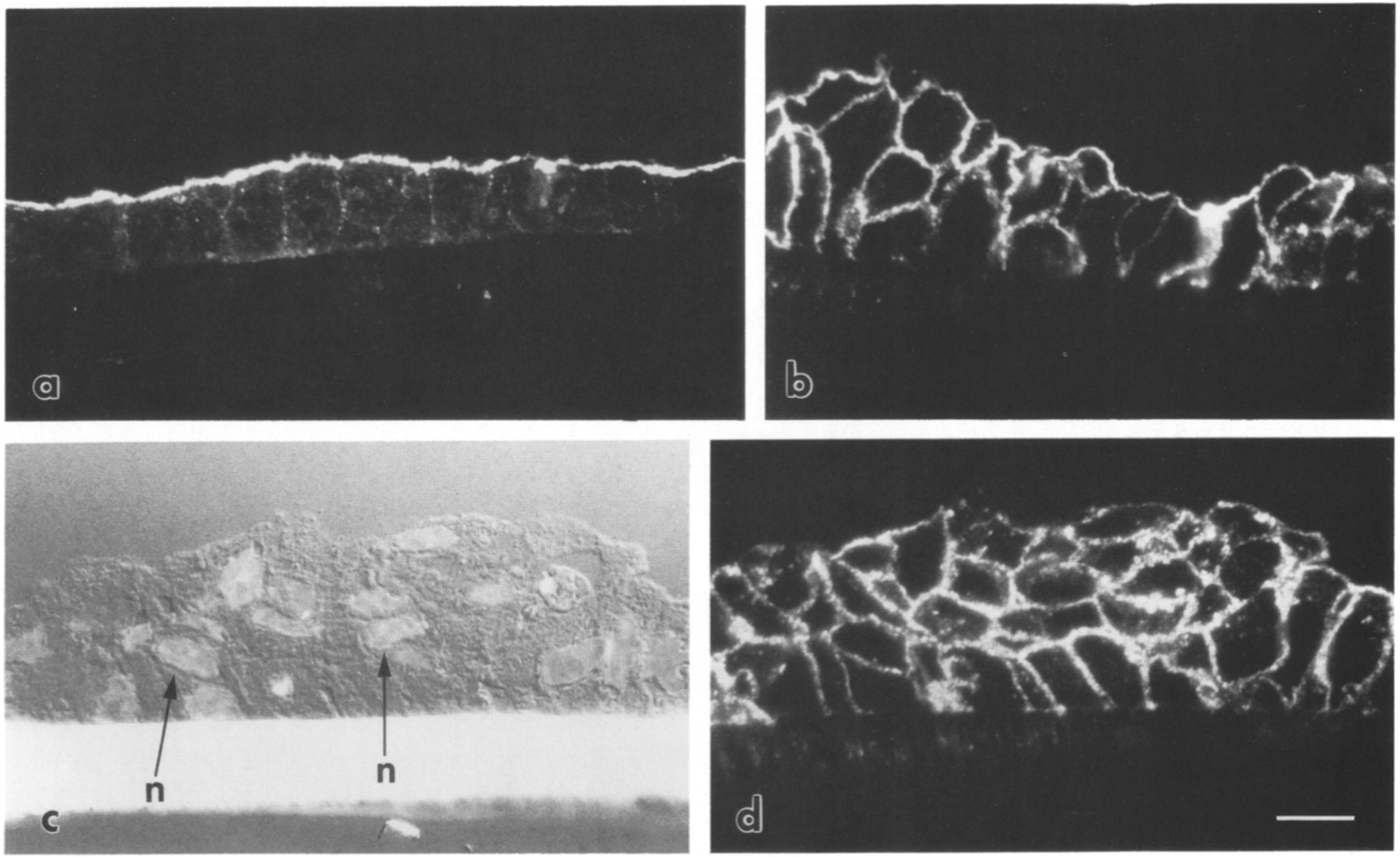

Figure 9. Randomized distribution of an apical 114-kD protein in R5 multilayers. Semi-thin cryosections of filter-grown C6 control and R5 transformed cells were stained by indirect immunofluorescence using an mAb to a 114-kD apical protein. (*a*) In C6 monolayers, the 114-kD protein is predominantly expressed on the apical surface and only minor staining is detectable along the basolateral membrane. (*b* and *d*) The normally apical 114-kD protein was distributed over the entire cell surface in multilayered R5 transformants. (*c*) Nomarski image of the multilayer shown in *d*, nuclei (*n*) counterstained with Hoechst. Bar, 10 μm.

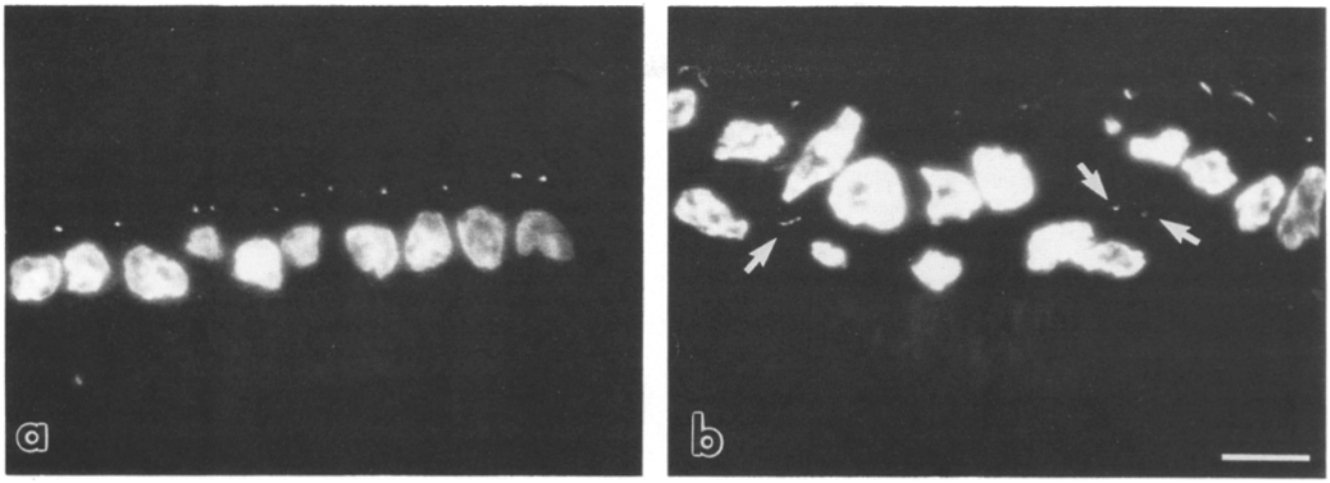

Figure 10. Immunolocalization of the tight junction specific protein ZO-1. Semi-thin cryosections of C6 control and R5 transformed filter-grown MDCK cells were stained by indirect immunofluorescence with mAbs to ZO-1. Nuclei were visualized by Hoechst staining. (*a*) In C6 monolayers, ZO-1 localized to discrete dots at the cell apex between neighboring cells. (*b*) In R5 multilayers, dot-like ZO-1 staining was apparent not only between adjacent cells facing the free surface, but also within the multilayer (*arrows*). Bar, 10 μm.

tribution of viral hemagglutinin over the cell surface (data not shown). Ultrastructural analysis confirmed that virions were budding in an unpolarized fashion. These findings presented further evidence that v-K-*ras* expression perturbed apical polarization in general and did not specifically affect the distribution of the 114-kD protein.

In summary, the immunofluorescence data suggested that the profound morphological changes accompanying transformation do not disrupt localization of basolateral proteins to areas of cell–cell contact. The random distribution of apical proteins in transformed cells corroborates the morphological observation that transformation abrogated the formation of a defined apical domain.

Disruption of Apical Polarity Does Not Interfere with the Establishment of Tight Junctions in Transformed MDCK Cells

In most epithelia tight junctions are positioned at the boundary between the apical and the basolateral domain. It has been reported that the localization of the tight junction protein ZO-1 to the apex of the lateral membrane in MDCK cells requires cell–substratum contact (Wang et al., 1990). Moreover, epithelial cells develop full polarity only after junctional complexes are established, suggesting that the formation of tight junctions is an important step in polarization (Gumbiner and Simons, 1986; Bacallao et al., 1990). To examine the formation of tight junctions in R5 multilayers, vertical cryosections were stained with monoclonal antibodies that recognize the tight junction-associated protein ZO-1 (Stevenson et al., 1986; Anderson et al., 1988). Immunolocalization of ZO-1 on semi-thin cryosections of control monolayers is shown in Fig. 10 *a*. The discrete punctate staining pattern reflects the ultrastructural appearance of tight junctions at the apex of lateral membranes between neighboring cells. In cryosections of R5 multilayers, dot-like ZO-1 staining was present not only at the boundary between the free and the apposed cell surface, but was also discernible within the multilayer (Fig. 10 *b*). These results indicated that the ZO-1 protein was associated with the plasma membrane at distinct sites although the apical polarity was disrupted in these cells.

The functional integrity of tight junctions in R5 multilayers was assessed by measuring the transepithelial resistance across the multilayer (Madara and Dharmsathaphorn, 1985; Madara and Hecht, 1989). In control monolayers a transepithelial resistance ranging from 45 to 55 $\Omega \cdot cm^2$ developed. These values were comparable with the transepithelial resistance measured across confluent monolayers of the parental MDCK clone. The transepithelial resistance in R5 multilayers was increased to 155–230 $\Omega \cdot cm^2$. In a monolayer, junctions can be viewed as individual resistors in parallel, each contributing to the total resistance. In comparison, the tight junctions in the additional cell layers of R5 cultures may act as resistors in series (Madara and Hecht, 1989). Therefore, it is possible that multilayering causes an increase in electrical resistance. Alternatively, transformation may have altered the electrical resistance of individual junctions.

The barrier formed by tight junctions to the paracellular transfer of small molecules can be assessed by measuring the flux of inulin across the cell layer (Madara and Dharmsathaphorn, 1985; Madara and Hecht, 1989). The rate of transfer of labeled ^{14}C-inulin from the apical compartment of filter cultures to the basal side revealed no significant difference between control and transformed MDCK cells (data not shown). The opening of the tight junctions by Ca^{2+} chelating EGTA-buffers affected monolayers and R5 multilayers similarly.

These findings suggested that R5 transformants establish tight junctions in multilayers. Despite the discrete localization of ZO-1 and the evidence of functional integrity, the tight junctions did not appear to restrict the distribution of the 114-kD apical surface marker to a defined plasma membrane domain. The randomized expression of the 114-kD protein over the entire cell surface in the presence of tight junctions indicated that polarization and tight junction formation are not correlated in transformed MDCK cells.

Discussion

In this paper we have demonstrated that oncogenic transformation of MDCK cells with the v-K-*ras* oncogene causes discrete changes in cell polarity and organization. In particular, we showed that transformants exhibit defective interaction with the substratum and abrogation of apical polarization while retaining functional tight junctions and localization of basolateral proteins to regions of cell–cell contacts. To our knowledge this is the first detailed analysis of the effects of transformation on the polarized epithelial phenotype.

Production of Transformants

The morphology of MDCK cells, like that of most other cell lines, spontaneously varies upon continuous passage. To ensure that oncogene expression and not morphological heterogeneity of the parental cell line accounted for the phenotypic changes in transformed MDCK cells, stocks of MDCK II cells were subcloned repeatedly before transformation. The acceptor line chosen exhibited morphological and growth characteristics nearly identical to the MDCK cells used previously in this laboratory (Matlin and Simons, 1983, 1984).

The retroviral vector pMV-7 provided a controlled method of introducing the *ras* oncogene. In general, retroviral vectors allow efficient gene transfer and stable integration of an intact viral genome. Unlike calcium phosphate–mediated DNA transfection methods in which an unpredictable number of copies is introduced, retroviral vectors usually insert one proviral copy into the host genome. Restriction enzyme analysis of transformant DNA confirmed that this was the case in this study, and also demonstrated that the integration site of the provirus differed between the transformed MDCK cell lines (data not shown).

Even more significantly, the pMV-7 retroviral vector transduces a selectable marker gene, thus permitting unbiased selection of transformants on the basis of antibiotic resistance rather than arbitrary morphological criteria. Oncogenically transformed cells are often selected as altered foci or as colonies able to grow in soft agar. Both of these criteria are prejudiced in favor of certain morphological phenotypes, since cells forming recognizable foci have aberrant shapes and tend to overgrow each other, while those that proliferate in soft agar must have changed adhesive characteristics. In contrast, the transformants described here were first selected randomly from a number of G418-resistant clones, and alterations in their organization determined subsequently.

Further evidence that phenotypic changes in transformed MDCK cells are a consequence of *ras* expression and not due to retroviral insertion was provided by infecting the parental cells with the pMV-7 retroviral vector lacking the oncogene insert. Without exception, these control lines displayed properties identical to those of the nontransformed parental cells.

Earlier efforts to produce transformed MDCK cells have not always controlled these various factors. MDCK cells transformed by infection with the Harvey murine sarcoma virus were selected as foci on the basis of morphological alterations rather than the presence of a transforming gene (Scolnick et al., 1976). Some foci gave rise to both epithelioid and fibroblastic clones (Darfler et al., 1986). Because the parental cell line was not clonal and is not available, it cannot be excluded that the original foci arose from several independently infected target cells.

Morphology of Transformed MDCK Cells

When grown on plastic substrata, all three transformed cell lines formed monolayers. Cell shapes were fairly cuboidal and reminiscent of normal epithelial cells. The most extensive deviation from normal morphology was seen in R5 cells. Rather than forming discrete colonies with smooth borders at low cell density, R5 cells had extensive processes and membrane ruffling indicative of changes in cell–cell and cell–substratum interactions. Even though R5 cells formed continuous monolayers, their saturation density was reduced, and dome formation did not occur. Because domes reflect the vectorial transport of solute (Valentich et al., 1979), their absence indicated that R5 cells might not be as polarized as normal MDCK cells. Fluorescent staining of lateral cell borders with the anti-114-kD antibody presented further evidence that the polarity in R5 cells grown on plastic substrata was compromised (unpublished observation).

MDCK cells which expressed high levels of v-*src* (Warren and Nelson, 1987) exhibited a phenotype similar to that of R5 cells. At low density these cells were spindly with extended processes. Upon reaching higher density, they adopted a more epithelial morphology once cell–cell contacts were established. However, in contrast to R5 cells, the *src* transformants formed atypical "polyps" which ultimately detached from the monolayer.

Much more dramatic changes in the organization of the transformants were evident when cells were grown on permeable supports. Under these conditions the transformants tended to form multilayers ranging from small clusters of cells in R2 to five layers of cells in R5. It has been reported that transformed mammary epithelial cells form bilayers when grown on collagen (Garcia et al., 1986). Why these differences in substratum have such an effect on the organization of transformed epithelial cells is not apparent. Permeable substrata and collagen gels permit nutrients and growth factors to more readily reach the basolateral surface of polarized epithelial cells. It has been speculated that this accessibility is conducive to epithelial differentiation (Simons and Fuller, 1985). In the case of transformed MDCK cells, altered cell adhesion seems to be promoted.

The formation of multilayers can be viewed from a different perspective by considering why epithelial cells grow in monolayers. In a monolayer, prevailing interactions with the substratum prevent cells from multilayering. Coupled with this is the fact that the apical surface is nonadherent; cells plated on top of a monolayer do not attach. When adherence to the substratum is reduced, then individual cells may adhere to each other. But for multilayering to ensue, the apical surface must also change to permit cell–cell adhesion.

Polarity of Transformed MDCK Cells

Ultrastructural analysis demonstrated that multilayered R5 cells have lost structural polarity. Normally, polarized epithelial cells are organized around an imaginary axis extending from the centrosome through the nucleus, perpendicular to the basal surface. Both the Golgi complex and the nucleus are positioned in specific locations with respect to this axis, with the Golgi supranuclear and the nucleus in a more basal location. In stratified epithelia, like epidermis, the defined apical–basal organization persists throughout multiple cell layers although cells of different layers may display specific

morphological features (Zelickson, 1967; Hay and Revel, 1969). In contrast, multilayers of R5 cells appear to have lost the orienting axis since the relative positions of the nuclei and Golgi complex bear no relationship to any defined surface.

In addition to these changes in cytoplasmic organization, immunocytochemical and ultrastructural data indicate that the apical surface is attenuated at best. On the free surface of the uppermost layer of cells, the number of microvilli is reduced, suggesting alterations in the subcortical cytoskeleton. Localization of normally apical proteins revealed that they were distributed randomly to not only the free surface of the uppermost cells and to intercellular lumina, but also to regions of cell–cell contact.

What was most striking, however, was that these major changes in cell organization were not accompanied by a complete loss of plasma membrane domains. A 58-kD basolateral protein was excluded from the free surface of the uppermost cell layer but was distributed over regions of the plasma membrane which, as ultrastructural analysis suggested, were involved in cell–cell contacts. The presence of the cell adhesion molecule uvomorulin in these regions was consistent with this interpretation. A similar localization of the Na^+,K^+-ATPase was also observed (unpublished results).

Polarization of some basolateral proteins in MDCK cells is related to the fodrin submembranous cytoskeleton (for review, see Nelson, 1989). According to a model developed primarily by Nelson and colleagues, uvomorulin and at least some basolateral membrane proteins interact with fodrin via association with ankyrin (Nelson and Veshnock, 1986, 1987*a*, *b*; Salas et al., 1988; Morrow et al., 1989; Nelson and Hammerton, 1989; Nelson et al., 1990). Homotypic cell–cell interactions mediated by uvomorulin apparently cause the reorganization and assembly of the submembranous cytoskeleton, constraining interacting proteins to the regions of cell–cell contacts. In transformed MDCK cells this mechanism appears to be intact, suggesting that altered cell–substratum interactions or lack of apical–basal organization do not interfere with the determinants of basolateral polarity. Moreover, the mechanisms that restrict basolateral proteins to areas of cell–cell contact do not exclude the apical 114-kD protein from these areas of contact.

The changes in cell organization brought about by transformation also affected the integrity of tight junctions only minimally. Measurements of electrical resistance and inulin flux across the R5 multilayer suggested that an intact barrier to solute flow existed. This conclusion was supported by the discrete dotlike localization of the tight junctional protein ZO-1 on frozen sections. These findings indicate that assembly and positioning of the tight junction occurs independently from the development of the apical domain. In addition, they demonstrate that while tight junctions may separate the apical and basolateral domains in polarized epithelial cells, their existence is not sufficient to ensure the formation of both apical and basolateral surfaces.

Tight junctions have been demonstrated to act as a fence, limiting diffusion of lipids in the outer leaflet of the plasma membrane (van Meer and Simons, 1986; van Meer et al., 1986). While they have not been shown to play a similar role with membrane proteins, it is difficult to imagine mechanisms that would permit diffusion of proteins through the junction while preventing the diffusion of lipids. Thus, in the case of the transformants, even though tight junctions function as barriers to the paracellular pathway, apical proteins are not restricted to any particular surface domain. This suggests that the initial targeting of apical proteins, which in MDCK cells occurs directly from the *trans*-Golgi network to the cell surface (Matlin and Simons, 1984; Caplan and Matlin, 1989), is defective in the transformants. Indeed, preliminary experiments indicate that sorting of viral hemagglutinin to the free surface is perturbed in R5 cells infected with influenza virus (unpublished observation).

ras and Polarization

Although we have not demonstrated a direct effect of the *ras* gene product on elements of the polarization machinery, it seems likely that the defects in cell–substratum interactions, cytoplasmic organization, and apical polarization are related to the expression of v-K-*ras*. The strongest evidence for this is that the transformed phenotypes of the three clones characterized here vary in proportion to the amount of v-K-*ras* mRNA and protein expressed. The p21-*ras* gene product is a GTP binding protein whose normal function in the cell is unknown. Recent results suggest the involvement of several *ras*-related GTP-binding proteins in membrane trafficking during exocytic and endocytic events (Chavrier et al., 1990). The findings reported here raise the possibility that p21-*ras* may be important for the spatial differentiation of epithelial cells.

If the effects of v-K-*ras* expression are specific, then one would expect that the phenotypes of epithelial cells transformed with other oncogenes would be distinctly different. Little data is available to confirm this supposition. In their studies of *src*-transformed MDCK cells, Warren and Nelson (1986) observed a defect in the ultrastructural appearance of the zonula adherens; however, cells forming cyst-like three-dimensional structures were morphologically polarized.

Biogenesis of Apical Polarity

As mentioned previously, basolateral polarization in MDCK cells depends on cell–cell contacts, most likely mediated by uvomorulin. Available data would suggest that apical polarization depends on both cell–substratum interactions and on cell–cell interactions. If MDCK cells are plated under conditions where cell–cell contacts do not form, then a rudimentary apical pole develops in the absence of basolateral polarization (Vega-Salas et al., 1987*a*,*b*; Ojakian and Schwimmer, 1988; Rodriguez-Boulan and Nelson, 1989; Wang et al., 1990). Upon formation of cell–cell contacts, the apical pole becomes fully developed. Taken at face value, these findings would seem to suggest that the organizational elements in the epithelial cell responsible for creation of the apical domain may be somewhat independent of those that make the basolateral domain.

We believe that our observations reported here are consistent with this hypothesis. Based on our findings we propose that the factors in the cell responsible for cell–substratum interactions, the positioning of organelles such as the Golgi complex, and the sorting of apical proteins are all related parts of the apical polarization machinery. Furthermore, this machinery operates independently of factors which organize the basolateral domain.

We are grateful to Dr. D. Louvard and Dr. J. Valentich for helpful discussions at the beginning of this work. We would also like to acknowledge

the assistance of the late Dr. I. Sigal of Merck Sharp and Dohme Research Laboratories. We thank Dr. J. L. Madara for his advice regarding inulin flux experiments. We also thank Dr. I. B. Weinstein for providing the pMV-7 vector, and Drs. J. B. Gibbs, M. Caplan, D. A. Goodenough, B. Gumbiner, and K. Simons for their kind gifts of antibodies. We are grateful to Dr. P. J. Hollenbeck for helpful criticisms of the manuscript.

This work was supported by grants CA-44331 and RR04951 to K. S. Matlin, and CA-08380 to A. Zuk from the National Institutes of Health. C.-A. Schoenenberger received a Swiss National Science Foundation Postdoctoral Fellowship.

Received for publication 10 September 1990 and in revised form 6 November 1990.

References

Abercrombie, M. 1980. The crawling movement of metazoan cells. *Proc. R. Soc. Lond. B. Biol.* 207:129–147.

Anderson, J. M., B. R. Stevenson, L. A. Jesaitis, D. A. Goodenough, and M. S. Mooseker. 1988. Characterization of ZO-1, a protein component of the tight junction from mouse liver and Madin-Darby canine kidney cells. *J. Cell Biol.* 106:1141–1149.

Bacallao, R., C. Antony, C. Dotti, E. Karsenti, E. H. K. Stelzer, and K. Simons. 1989. The subcellular organization of Madin-Darby canine kidney cells during the formation of a polarized epithelium. *J. Cell Biol.* 109: 2817–2832.

Balcarova-Ständer, J., S. E. Pfeiffer, S. D. Fuller, and K. Simons. 1984. Development of cell surface polarity in the epithelial Madin-Darby canine kidney (MDCK) cell line. *EMBO (Eur. Mol. Biol. Organ.) J.* 3:2687–2694.

Ball, R. K., A. Ziemiecki, C.-A. Schoenenberger, E. Reichman, S. M. S. Redmond, and B. Groner. 1988. V-*myc* alters the response of a cloned mouse mammary epithelial cell line to lactogenic hormones. *Mol. Endocrinol.* 133–142.

Barbacid, M. 1987. *ras* genes. *Annu. Rev. Biochem.* 56:779–827.

Behrens, J., W. Birchmeier, S. L. Goodman, and B. A. Imhof. 1985. Dissociation of Madin-Darby canine kidney epithelial cells by the monoclonal antibody anti-arc-1: mechanistic aspects and identification of the antigen. *J. Cell Biol.* 101:1307–1315.

Behrens, J., M. M. Mareel, F. M. VanRoy, and W. Birchmeier. 1989. Dissecting tumor cell invasion: epithelial cells acquire invasive properties after the loss of uvomorulin-mediated cell-cell adhesion. *J. Cell Biol.* 108:2435–2447.

Berridge, M. J., and J. L. Oschman. 1972. Transporting epithelia. Academic Press, New York. pp. 91–108.

Bramhall, S., N. Noack, M. Wu, and J. R. Lowenberg. 1969. A simple colorimetric method for the determination of protein. *Anal. Biochem.* 31:146–148.

Burke, B., G. Griffiths, H. Reggio, D. Louvard, and G. Warren. 1982. A monoclonal antibody against a 135-K Golgi membrane protein. *EMBO (Eur. Mol. Biol. Organ.) J.* 1:1621–1628.

Caplan, M., and K. S. Matlin. 1989. Sorting of membrane and secretory proteins in polarized epithelial cells. *In* Functional Epithelial Cells in Culture. K. S. Matlin and J. D. Valentich, editors. Alan R. Liss, Inc., New York. 71–127.

Caplan, M. J., H. C. Anderson, G. E. Palade, and J. D. Jamieson. 1986. Intracellular sorting and polarized cell surface delivery of (Na^+,K^+)ATPase, an endogenous component of MDCK cell basolateral plasma membranes. *Cell.* 46:623–631.

Cereijido, M., I. Meza, and A. Martinez-Palomo. 1981. Occluding junctions in cultured epithelial monolayers. *Am. J. Physiol.* 240:C96–C102.

Chavrier, P., R. G. Parton, H.-P. Hauri, K. Simons, and M. Zerial. 1990. Localization of low molecular weight GTP binding proteins to exocytic and endocytic compartments. *Cell.* 62:317–329.

Chirgwin, J. M., A. E. Przybyla, R. J. MacDonald, and W. J. Rutter. 1979. Isolation of biologically active ribonucleic acid from sources enriched in ribonuclease. *Biochemistry.* 18:5294–5299.

Darfler, F. J., T. Y. Shih, and M. C. Lin. 1986. Revertants of Ha-MuSV-transformed MDCK cells express reduced levels of p21 and possess a more normal phenotype. *Exp. Cell Res.* 162:335–346.

Davis, L. G., M. D. Dibner, and J. F. Battey. 1986. Preparation of RNA from eukaryotic cells. *In* Basic Methods in Molecular Biology. Elsevier/North Holland, New York. 129–146.

Ekblom, P. 1989. Developmentally regulated conversion of mesenchyme to epithelium. *FASEB (Fed. Am. Soc. Exp. Biol.) J.* 3:2141–2150.

Ellis, R. W., D. DeFeo, T. Y. Shih, M. A. Gonda, H. Z. A. Yound, N. Tsuchida, D. R. Lowry, and E. M. Scolnick. 1981. The p21 *src* genes of Harvey and Kirsten sarcoma viruses originate from divergent members of a family of normal vertebrate genes. *Nature (Lond.).* 292:506–511.

Farquahr, M. G., and G. E. Palade. 1963. Junctional complexes in various epithelia. *J. Cell Biol.* 17:375–412.

Fawcett, D. W. 1986. A Textbook of Histology. W. B. Saunders Co., Philadelphia. 57–72.

Flemming, T. P., and M. H. Johnson. 1988. From egg to epithelium. *Annu. Rev. Cell Biol.* 4:459–485.

Fuller, S. D., and K. Simons, 1986. Transferrin receptor polarity and recycling accuracy in "tight" and "leaky" strains of Madin-Darby kidney cells. *J. Cell Biol.* 103:1767–1779.

Furth, M. E., L. J. Davis, B. Fleurdelys, and E. M. Scolnick. 1982. Monoclonal antibodies to the p21 products of the transforming gene of Harvey murine sarcoma virus and of the cellular *ras* gene family. *J. Virol.* 43:294–304.

Garcia, I., B. Sordat, E. Rauccio-Farinon, M. Dunand, J.-P. Kraehenbuhl, and H. Diggelman. 1986. Establishment of two rabbit mammary epithelial cell lines with distinct oncogenic potential and differentiated phenotype after microinjection of transforming genes. *Mol. Cell. Biol.* 6:1974–1982.

Graham, F. L., and A. J. van der Eb. 1973. A new technique for the assay of infectivity of human adenovirus 5 DNA. *Virology.* 52:456–467.

Gumbiner, B. 1987. Structure, biochemistry, and assembly of epithelial tight junctions. *Am. J. Physiol.* 5922:C749–758.

Gumbiner, B., and K. Simons. 1986. A functional assay for proteins involved in establishing an epithelial occluding barrier: identification of a uvomorulin-like polypeptide. *J. Cell Biol.* 102:457–468.

Gumbiner, B., B. Stevenson, and A. Grimaldi. 1988. The role of the cell adhesion molecule uvomorulin in the formation and maintenance of the epithelial junctional complex. *J. Cell Biol.* 107:1575–1588.

Handler, J. S., A. S. Preston, and R. E. Steele. 1984. Factors affecting the differentiation of epithelial transport and responsiveness to hormones. *Fed. Proc.* 43:2221–2224.

Hay, E. D., and J.-P. Revel. 1969. Fine Structure of the Developing Cornea. S. Karger, Basel, Switzerland.

Hertzlinger, D. A., and G. K. Ojakian. 1984. Studies on the development and maintenance of epithelial cell surface polarity with monoclonal antibodies. *J. Cell Biol.* 98:1777–1787.

Kirschmeier, P. T., G. M. Housey, M. D. Johnson, A. S. Perkins, and I. B. Weinstein. 1988. Construction and characterization of a retroviral vector demonstrating efficient expression of cloned cDNA sequences. *DNA (NY).* 7:219–225.

Laemmli, U. K. 1970. Cleavage of structural proteins during the assembly of the head of bacteriophage T4. *Nature (Lond.)* 227:683–685.

Louvard, D. 1980. Apical membrane aminopeptidase appears at site of cell-cell contact in cultured kidney epithelial cells. *Proc. Natl. Acad. Sci. USA.* 77:4132–4136.

Madara, J. L., and K. Dharmsathaphorn. 1985. Occluding junction structure-function relationships in a cultured epithelial monolayer. *J. Cell Biol.* 101: 2124–2133.

Madara, J. L., and G. Hecht. 1989. Tight (occluding) junctions in cultured (and native) epithelial cells. *In* Functional Epithelial Cells in Culture. K. S. Matlin and J. D. Valentich, editors. Alan R. Liss, Inc., New York. 131–163.

Maniatis, T., E. F. Fritsch, and J. Sambrook. 1982. Molecular Cloning: A Laboratory Manual. Cold Spring Harbor Laboratory, Cold Spring Harbor, NY. 545 pp.

Matlin, K. S., and K. Simons. 1983. Reduced temperature prevents transfer of a membrane glycoprotein to the cell surface but does not prevent terminal glycosylation. *Cell.* 34:233–243.

Matlin, K. S., and K. Simons. 1984. Sorting of an apical plasma membrane glycoprotein occurs before it reaches the cell surface in cultured epithelial cells. *J. Cell Biol.* 99:2131–2139.

McLean, I. W., and P. K. Nakane. 1977. Periodate-lysine-paraformaldehyde fixative. A new fixative for immunoelectron microscopy. *J. Histochem. Cytochem.* 22:1077–1081.

McNeill, H., M. Ozawa, R. Kemler, and W. J. Nelson. 1990. Novel function of the cell adhesion molecule uvomorulin as an inducer of cell surface polarity. *Cell.* 62:309–316.

Miller, A. D., and C. Buttimore. 1986. Redesign of retrovirus packaging cell lines to avoid recombination leading to helper virus production. *Mol. Cell Biol.* 6:2895–2902.

Morrow, J. S., C. D. Cianci, T. Ardito, A. S. Mann, and M. Kashgarian. 1989. Ankyrin links fodrin to the alpha subunit of Na,K,-ATPase in Madin-Darby canine kidney cells and in intact renal tubule cells. *J. Cell Biol.* 108:455–465.

Nelson, W. J. 1989. Development and maintenance of epithelial polarity: a role for the submembranous cytoskeleton. *In* Functional Epithelial Cells in Culture. K. S. Matlin and J. D. Valentich, editors. Alan R. Liss, Inc., New York. 3–42.

Nelson, W. J., and P. J. Veshnock. 1986. Dynamics of membrane-skeleton (fodrin) organization during development of polarity in Madin-Darby canine kidney epithelial cells. *J. Cell Biol.* 103:1751–1766.

Nelson, W. J., and P. J. Veshnock. 1987*a*. Modulation of fodrin (membrane skeleton) stability by cell-cell contact in Madin-Darby canine kidney epithelial cells. *J. Cell Biol.* 104:1527–1537.

Nelson, W. J., and P. J. Veshnock. 1987*b*. Ankyrin binding to (Na^+,K^+)ATPase and implications for the organization during development of membrane domains in polarized cells. *Nature (Lond.).* 328:533–536.

Nelson, W. J., and R. W. Hammerton. 1989. A membrane-cytoskeletal complex containing Na^+,K^+-ATPase, ankyrin, and fodrin in Madin-Darby canine kidney (MDCK) cells: implications for the biogenesis of epithelial cell polarity. *J. Cell Biol.* 108:893–902.

Nelson, W. J., E. M. Shore, A. Z. Wang, and R. W. Hammerton. 1990.

Identification of a membrane-cytoskeletal complex containing the cell adhesion molecule uvomorulin (E-cadherin), ankyrin, and fodrin in Madin-Darby canine kidney epithelial cells. *J. Cell Biol.* 110:349–357.

Nicolson, G. L. 1989. Metastatic tumor cell interactions with endothelium, basement membrane and tissue. *Curr. Op. Cell Biol.* 1:1009–1019.

Ojakian, G. K., and R. Schwimmer. 1988. The polarized distribution of an apical cell surface glycoprotein is maintained by interactions with the cytoskeleton of Madin-Darby canine kidney cells. *J. Cell Biol.* 107:2377–2387.

Parry, G., B. Cullen, C. S. Kaetzel, R. Kramer, and L. Moss. 1987. Regulation of differentiation and polarized secretion in mammary epithelial cells maintained in culture: extracellular matrix and membrane polarity influences. *J. Cell Biol.* 105:2043–2051.

Powell, D. W. 1981. Barrier function of epithelia. *Am. J. Physiol.* 241:G275–G288.

Redmond, S. M. S., E. Reichman, R. G. Müller, R. R. Friis, B. Groner, and N. E. Hynes. 1988. The transformation of primary and established mouse mammary epithelial cells by p21-*ras* is concentration dependent. *Oncogene.* 2:259–265.

Rijsewijk, F., L. van Deemter, A. Wagenaar, A. Sonnenberg, and R. Nusse. 1987. Transfection of the *int*-1 mammary oncogene in cuboidal RAC mammary cell line results in morphological transformation and tumorigenicity. *EMBO (Eur. Mol. Biol. Organ.) J.* 6:127–131.

Rodriguez-Boulan, E., and D. D. Sabatini. 1978. Asymmetric budding of viruses in epithelial monolayers: a model system for study of epithelial polarity. *Proc. Natl. Acad. Sci. USA.* 75:5071–5075.

Rodriguez-Boulan, E., and W. J. Nelson. 1989. Morphogenesis of the polarized epithelial cell phenotype. *Science (Wash. DC).* 245:718–725.

Salas, P. J. I., D. E. Vega-Salas, J. Hochman, E. Rodriguez-Boulan, and M. Edidin. 1988. Selective anchoring in the specific plasma membrane domain: a role in epithelial cell polarity. *J. Cell Biol.* 107:2363–2376.

Scolnick, E. M., D. Williams, J. Maryak, J. Vass, R. J. Goldberg, and W. P. Parks. 1976. Type C particle-positive and type C particle-negative rat cell lines: characterization of the coding capacity of endogenous sarcoma virus-specific RNA. *J. Virol.* 20:570–582.

Simons, K., and S. D. Fuller. 1985. Cell surface polarity in epithelia. *Annu. Rev. Cell Biol.* 1:243–288.

Stevenson, B. R., J. D. Siliciano, M. S. Mooseker, and D. A. Goodenough. 1986. Identification of ZO-1: a high molecular weight polypeptide associated with the tight junction (zonula occludens) in a variety of epithelia. *J. Cell Biol.* 103:755–766.

Stiles, C. D., W. Desmond, L. M. Chuman, G. Sato, and M. H. Saier, Jr. 1976*a*. Growth control of heterologous tissue culture cells in the congenitally athymic nude mouse. *Cancer Res.* 36:1353–1360.

Stiles, C. D., W. Desmond, L. M. Chuman, G. Sato, and M. H. Saier, Jr. 1976*b*. Relationship of cell growth behavior *in vitro* to tumorigenicity in athymic nude mice. *Cancer Res.* 36:3300–3305.

Valentich, J. D. 1982. Basal-lamina assembly by the dog kidney cell line MDCK. *Cold Spring Harbor Conf. Cell Prolif.* 9:567–579.

Valentich, J. D., R. Tchao, and J. Leighton. 1979. Hemicyst formation stimulated by cyclic AMP in dog kidney cell line MDCK. *J. Cell. Physiol.* 100:291–304.

van Meer, G., and K. Simons. 1986. The function of tight junctions in maintaining differences in lipid composition between the apical and the basolateral cell surface domains of MDCK cells. *EMBO (Eur. Mol. Biol. Organ.) J.* 5:1455–1464.

van Meer, G., B. Gumbiner, and K. Simons. 1986. The tight junction does not allow lipid molecules to diffuse from one epithelial cell to the next. *Nature (Lond.)* 322:639–641.

Vega-Salas, D. E., P. J. I. Salas, D. Gundersen, and E. Rodriguez-Boulan. 1987*a*. Formation of the apical pole of epithelial (Madin-Darby canine kidney) cells: polarity of an apical protein is independent of tight junctions while segregation of a basolateral marker requires cell-cell interactions. *J. Cell Biol.* 104:905–916.

Vega-Salas, D. E., P. J. I. Salas, and E. Rodriguez-Boulan. 1987*b*. Modulation of the expression of an apical plasma membrane protein of Madin-Darby canine kidney epithelial cells: cell-cell interactions control the appearance of a novel intracellular storage compartment. *J. Cell Biol.* 104:1249–1259.

Wang, A. Z., G. K. Ojakian, and W. J. Nelson. 1990. Steps in the morphogenesis of a polarized epithelium. I. Uncoupling the roles of cell-cell and cell-substratum contact in establishing plasma membrane polarity in multicellular epithelial (MDCK) cysts. *J. Cell Sci.* 95:137–151.

Warren, S. L., and W. J. Nelson. 1987. Nonmitogenic morphoregulatory action of $pp60^{v\text{-}src}$ on multicellular epithelial structures. *Mol. Cell. Biol.* 7:1326–1337.

Wigler, M., R. Sweet, G. K. Sim, B. Wold, E. Lacy, T. Maniatis, S. Silverstein, and R. Apel. 1979. Transformation of mammalian cells with genes from procaryotes and eukaryotes. *Cell.* 16:777–785.

Willingham, M. C., I. Pastan, T. Y. Shih, and E. M. Scolnick. 1980. Localization of the *src* gene product of the Harvey strain of MSV to plasma membrane of transformed cells by electron microscopic immunocytochemistry. *Cell.* 10:1005–1014.

Wilson, E. B. 1987. The cell in development and heredity. Reprint of third edition of 1928. Garland Publishing Inc., New York. 106–111.

Zelickson, A. S. 1967. Ultrastructure of Normal and Abnormal Skin. Lea & Febiger, Philadelphia.